UNIVERSIDAD AUTÓNOMA DE SAN LUIS POTOSI

DOCTORADO INSTITUCIONAL EN INGENIERIA Y CIENCIA DE LOS MATERIALES

Relaxation of Residual Stresses in Plastic Cover Lenses with Applications in the Injection Molding Process

THESIS REQUERIMENT TO GET THE DEGREE

DOCTORADO EN INGENIERIA Y CIENCIA DE LOS MATERIALES

BY

M. Eng. CESAR OCTAVIO MACIAS GONZALEZ

A D V I S O R S

DR. JOSÉ ELÍAS PÉREZ LÓPEZ

DR. LUIS OCTAVIO MEZA ESPINOZA

San Luis Potosí, S.L.P.

ACKNOWLEDGMENTS

TO MY BELOVED FAMILY

I like to express my deepest gratitude to my wife Julieta and my baby César Mateo, for their unconditional love and support during my studies and finalization of this important stage in our life.

I want to thank my parents, brothers and sister because they encouraged me to continues with this studies.

A very special recognition needs to be given to my advisor Dr. Elías Pérez and Dr. Octavio Meza, this thesis could not have been written without his guidance and supervision in all the moments of this postgraduate studies.

I would like to acknowledge warmly to my friend Guillermo Maldonado for his encourage to start with this new challenge.

Finally, I need to acknowledge to my colleagues from Czech Republic, especially to Dr. Brodinova who during my stance in this country support me always with the tools in her lab in order to continue with my investigation.

Contents

Chapter I 9

Introduction 9

1.1. Statement of the Problem and Motivation 9

1.2. Scientific Approach 10

Chapter II 12

Background 12

2.1. State of the art 12

2.2. Flow behavior of polymeric fluids 14

2.3. Orientation, relaxation and shrinkage 19

2.4. Glass Transition Temperature **Tg** 22

2.4. Residual Stress in Thermoplastics Parts 23

2.4.1. Nondestructive method of residual stress measurement 25

2.4.2. Photoelasticity Technique 26

2.4.3. Fundamental Optical Laws of Photoelasticity 30

2.4.4. Polariscope Arrangement 31

2.4.5. Design of Experiments (DOE) 34

Chapter III 36

Experimental Methodology 36

3.1. Bulk Samples Preparation 36

3.2. Experimental Stress Analysis 38

3.3. Experimental Stress Analysis: Destructive Characterization 38

3.4. Experimental Stress Analysis: Nondestructive Characterization 41

Chapter IV 45

Results and Discussion 45

4.1 Preliminary analysis of testing results 45

4.2 Testing results of the polarized light 46

4.3 Testing results of the chemical attack 47

4.4 Testing results after heat treatment 49

4.5 Testing results of image processing 52

Chapter V 61

Conclusion and Future Work 61

Biographical Sketch 67

Annex I 68

LIST OF FIGURES

Figure **Page**

Figure 1, Qualitative behavior of the steady shear viscosity of polymeric fluids (13)..... 16

Figure 2, The effect of shear on the viscosity polymeric materials: low Newtonian plateau (I), power law region (II), and upper Newtonian plateau (III). 17

Figure 3, Simple shear flow between parallel plates 18

Figure 4, Typical **pvT** curves for: (a) amorphous and (b) semicrystalline polymers. 20

Figure 5, (a) Random coil, (b) Flow-induced orientation, (c) Uniaxial orientation, (d) Biaxial orientation..... 21

Figure 6, Temperature dependence of the specific volume of amorphous polymer. 22

Figure 7, Relationship between elastic modulus and temperature (5)..... 23

Figure 8, Ordinary Light –No control over light vector 26

Figure 9, Plane polarization 27

Figure 10, The electromagnetic spectrum. 27

Figure 11, Mathematical representation of light wave (16). 28

Figure 12, Optical equipment arrangement, a) plane polariscope, b) plane polariscope including compensator to obtain the values of $\boldsymbol{\delta}$. 32

Figure 13, Model in a plane polariscope 33

Figure 14, The engineering method. Steps 2–4, are enclosed in a box, indicating that several cycles or iterations of these steps may be required to obtain the final solution..... 34

Figure 15, 3DSolid model of PCL's injection molding tool cavity 37

Figure 16, Plastic cover lens subject to analysis 37

Figure 17, Test medium reaction threshold for testing of parts produced with Makrolon® (11). 39

Figure 18, Stress crack test under load to DIN EN ISO 22088-2. Tensile creep method on medium viscosity Makrolon® (11). 40

Figure 19, Polariscope used in this work which consists of light source L, and polarizator P.. 41

Figure 20, Plastic cover lens analyzed under polarized light where streamlines are detected close to the gate 42

Figure 21, Section of plastic cover lens under polarized light 42

Figure 22, Shown the compensator LWC-100 used to determine the retardation value. 43

Figure 23, a) sample under polarized light without heat treatment, b) partial crack, c) complete crack of sample real view on PCL..... 46

Figure 24. Initial crack originated due to concentration of residual stress where boss is located in the dome..... 46

Figure 25, Determination of fringe orders during qualitative analysis 47

Figure 26, Sample subject to chemical attack by propylene carbonate which cause stress-cracking 48

Figure 27, Residual stress magnitude determined as a function of time using chemical attack which causes crack. 48

Figure 28, Comparison of results obtained by photoelasticity and chemical attack experiments..... 49

Figure 29, Section of the sample after BFHA at 110°C and 5 minutes of heat treatment in the laboratory..... 53

Figure 30, Section of the sample after BFHA at 110°C and 5 minutes processed by MATLAB®. 54

Figure 31, Plot main effects of each predictor in the linear regression model..... 57

Figure 32, Relaxation of residual stresses as function of [time & temperature]. 57

LIST OF TABLES

Table **Page**

Table 1, Typical Shear Rates for Selected Processes 18

Table 2, Processing conditions used for injection molding..... 38

Table 3, Heat treatment process of samples under analysis, using different parameters for temperature and time..... 50

Table 4, DOE of annealing process 51

Table 5, Hypothesis tests of proportions for annealing process by CFHA..... 52

Table 6, Quantitative analysis of residual stresses on samples used in the DOE by image processing. 55

Table 7, Analysis of variance for residual stresses 56

Abstract of Thesis Presented to the Graduate School of the
Autonomous University of San Luis Potosi Fulfillment of the
Requirements for the Degree of Doctorate in Engineering and Material Science

Relaxation of Residual Stresses in Plastic Cover Lenses with Applications in the Injection Molding Process

Plastic cover lenses (PCLs) made of polycarbonate (PC) are widely used nowadays in the automotive industry due to guarantee good performance, dimensional stability, resistance to different work environment, lightweight, ductility, low cost compared with glasses and saving of fuel consuming mainly in automobiles.

The present thesis is concerned to the injection molding process (IMP) an irreversible process where polymer change from solid to melt state and after cooling process it solidified in a desired specific geometry. In this work we analyze how mechanical and optical properties are affected at the end of the IMP by flow-induced residual stresses originated due to the complex path that the flow follows through mold cavities of injection mold.

The study of residual stresses was conducted on plastic parts made of amorphous polycarbonate AL 2447. This study include two measurement techniques to determine the residual stress on transparent parts: birefringence and chemical attack methods, first one defined a non-destructive characteristic and second one a destructive technique. The magnitude of this non-desired characteristic was determined by these two methods and a stress-relieving technique was successfully implemented by annealing process, the parameters of this technique were optimized and determined in the environmental test laboratory based on previous analysis of

factors and levels by a design of experiments (DOE). This DOE was conducted considering several physical properties of this amorphous polycarbonate.

Chapter I

Introduction

1.1.Statement of the Problem and Motivation

Research in polymers science continues growing and the amount of secondary engineering products of polymers as well; however the real challenge comes when those polymeric materials are being used to produce an end product using different technologies, where most of the polymeric materials are processed by injection molding process.

Nowadays plastic cover lenses are widely used in headlights due to their advantages in terms of physical properties and performance in comparison with glass panes. The lower cost of production, the influence on fuel consumption, and in consequence the CO_2 emissions by automobiles are among the most important considerations in replacing the use of glass panes with polycarbonate PCLs. PCLs are manufactured by an injection molding process (IMP), which is a high-speed automated process that is used to produce plastic parts with very complex geometries at relatively low cycle times. This process involves a series of sequential process steps: mold filling, packaging, holding, cooling, and part ejection. In this complex process, a real challenge is keeping the quality of the raw material's properties when it has undergone the physical change from solid to melted material and finally transformed into a stable PCL. A major problem frequently encountered occurs during surface finish process of PCLs. This process consisted in the application of a hard coating layer

on inner and outer lens surface, a process which is necessary to protect the PCL's surface from media that cause degradation of polycarbonate properties due to ultraviolet radiation (UV), abrasion, and different environmental conditions, and this finish is decisive because it provides an effective diffusion barrier against these physical phenomenon; however in some cases the hard coating layer application reveals where the residual stresses are located in the microstructural ordering of PCL and causes stress-cracking.

1.2.Scientific Approach

The quality of molded parts made of clear thermoplastic polymers is determined by the absence or presence of residual stresses. In this work we analyzed the flow-induced residual stresses, which cause serious damage to plastic parts used in automotive and optical applications. Plastic cover lenses (PCLs) are important components of LED and bulb headlights that are produced by the injection molding process (IMP). However due to multiple characteristics of PCLs as, complex geometry, size and wall thickness residual stresses are difficult to keep under control during the IMP, causing cracking under chemical attack, ultraviolet radiation, abrasion and other environmental conditions. These residual stresses in PCLs were characterized by a chemical attack and photoelasticity method in the present work, and the methods were compared and validated. A stress-relieving technique was then successfully applied, implementing a thermal treatment for prototypes, and after its validation in the laboratory it was applied in a series production. These experiments were based on

a design of experiments (DOE) for the annealing process considering the glass transition temperature (Tg) of the polycarbonate and allowing the relaxation of the internal microstructure of PCLs without causing degradation, helping us to increase the production efficiency and improve the component performance in the plant.

Chapter II

Background

In this chapter is presented a brief summary of the principles in which was based the analysis of this work basically theoretical and mathematical concepts in order simplify the understanding of the next chapters in which will present results and discussions. This chapter will cover topics as non-Newtonian melt flow, optical theory and testing-failure analysis of plastics.

The purpose of the summary in some topics, it is not intended to cover the background of research in their entirety, but rather to present a work-frame for the rest of this work.

2.1.State of the art

Residual stress is one of the major problems in the injection molding process. It is clear that a right understanding of residual stresses is essential to predict the dimensional and shape stability of a product under different environmental conditions (2). The origin of the residual stresses is associated with two sources. Firstly, the normal stress in the molding process is originated by the viscoelastic nature of the polymeric melt that develops during the filling, packing, and holding states. This normal force is relatively small but is important for large molecular orientations that occur in the PCL injection process. Secondly, thermally induced stresses are originated by non-uniform cooling in the molding part. This last

phenomenon takes place due to a rapid increase in the rigidity of the material as it passes through the glass transition temperature, Tg; as a consequence, a highly non-uniform temperature distribution exists across the product wall (2; 3; 4; 5). Investigations by Zhang et al. (6), predicted thermally induced residual stresses that form during the injection molding using an approximate model and found how the residual stress in an IMP is affected by process conditions and material properties based on a model of solidification (mold–solid-layer–fluid). Residual stresses have already been studied by different authors: Postawa (7), studied the residual stress distribution in injection molding parts made of polystyrene (PS), using the monochromatic photoelasticity technique for different processing parameters for the qualitative estimation of internal stresses. It was found that the most important variables were a low hold pressure and a high injection temperature. On the other hand, Can Weng (8) studied the presence of residual tresses in micro-lens arrays using the birefringence method to evaluate the residual stresses and finite element simulations to estimate their distribution. Comparable results from both experiments are correlated and the most important process parameter is the mold temperature. These studies revealed that the molding process parameters are highly correlated with the origin of residual stresses and the most important variables are the melt temperature, T_f, mold temperature, T_w, packaging pressure, P_p, holding pressure, P_h, filling time, F_t, cooling time, t_{ch}, and velocity of the flow in cavity, V_i, or in some cases the tool design, T_D. These residual stresses cause serious damage to PCLs when they are exposed to different environmental conditions. Jacques (9), investigated the susceptibility of glassy polymers to cracking when exposed to gasoline with different

percentages of aromatic composition, where polycarbonate PC, polymethyl methacrylate PMMA, and cellulose acetate butyrate CAB have different threshold reactions, influenced by geometrical factors and reduced critical strain; however the use of a specific test medium can be useful to determine the concentration of the residual stresses in PCLs. The use of non-destructive methods is one of the most important techniques for actually determining the residual stress in transparent plastics and glass. Yeager (10) analyzed specific areas of plastic parts to determine the residual stresses, using a compensator to find the retardation value for a PC involving the Brewster's constant and other physical properties of material for a commercial polycarbonate, Makrolon. Bayer Material Science (11), published studies about stress crack tests for commercial PC-Makrolon, which has been tested with different media regarding the use of the part subjected to mechanical stresses. The main objective of this paper is the analysis of the flow-induced residual caused by IMP.

The use of chemical attack and photoelasticity methods shows comparable results, which were correlated with a previous qualitative analysis by photoelasticity carried out to detect areas of PCLs subject to failure due to residual stresses. Finally a stress-relieving technique was successfully applied, implementing a thermal treatment for prototypes samples, and after its validation it was applied in series production as quality control in the plant.

2.2.Flow behavior of polymeric fluids

Polymers owe their attractiveness as material for a wide range of applications to a large extent to their ease of processing. Manufacturing processes such as injection

molding, fiber spinning of film formation are mainly conducted in the melt and it is a great advantage of polymers that their melting temperatures are comparatively low. On the other hand, the flow properties of polymer melts are complicated and process control requires abroad knowledge. To deal with simple Newtonian liquids, one needs just only one parameter, namely the viscosity, η. In principle, knowing it allows us to calculate stresses for any given flow pattern. Polymeric liquids are more complex in behavior. From the very beginning, i.e., even at low frequencies or low shear rates; one has to employ two coefficients for a characterization. They are shear viscosity and recoverable shear compliance, J_e, that relates to the always present elastic forces. At higher strain rates more complications arise. Is known that η is the property of the resistance to flow exhibited within a body of material (1). Ordinary viscosity is the internal friction or resistance of a plastic to flow. It is the constant ratio of shearing stress to the rate shear. Shearing is the motion of a fluid, layer by layer, like a deck of cards. When plastics flow through straight tubes or channels they are sheared and the viscosity expresses their resistance. The melt index (MI) or melt flow index (MFI) is an inverse measure of viscosity. High MI implies low viscosity and low HI means high viscosity. Plastics are shear tinning, which means that their resistance to flow decrease as the shear rate increase. This is due to molecular alignment in the direction of flow and disentanglements. Viscosity is usually understood to mean Newtonian viscosity, in which case the ratio of shearing strain is constant. In non-Newtonian behavior, which is the usual case for plastics, the ratio varies with the shearing stress. Such ratios are often called the apparent viscosities at the corresponding shear stresses. Viscosity is usually measured in terms of flow in (Pas), (equivalent to

(N.s)/m^2), with water as the base standard (value of 1.0). The higher number, the less flow.

Newtonian flow if a material (liquid, etc.) flows immediately on application of force and the rate of flow is directly proportional to the force applied the flow is Newtonian. It is a flow characteristic evidenced by viscosity that is independent of shear rate.

Non-Newtonian flow. There are some plastics melts or liquids that exhibit non-Newtonian flow response when force is applied. That is, their viscosity depends on the rate of shear. Deviations from ideal Newtonian behavior may be of several different types.

One type is attributed to apparent viscosity, which may increase with shear rate (shear thickening or shear dilatancy) or decrease with rate of shear (shear thinning or pseudoplasticity). The latter behavior is usually found with plastic melts and solutions. In general such a dependency of shear stress on shear rate can be expressed as a power law (12).

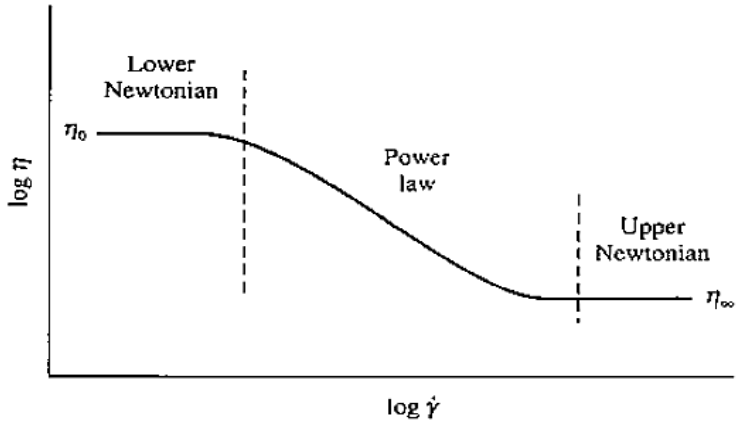

Figure 1, Qualitative behavior of the steady shear viscosity of polymeric fluids **(13)**

As shown in the Figure 2, de decrease in the viscosity of pseudoplastic fluids does not occur immediately. At lower shear rates, the polymer molecules flow as random coils and the viscosity of polymer melt is not affected by increasing the shear rate. The constant viscosity of this lower Newtonian plateau is called the zero shear-rate viscosity, η_0.

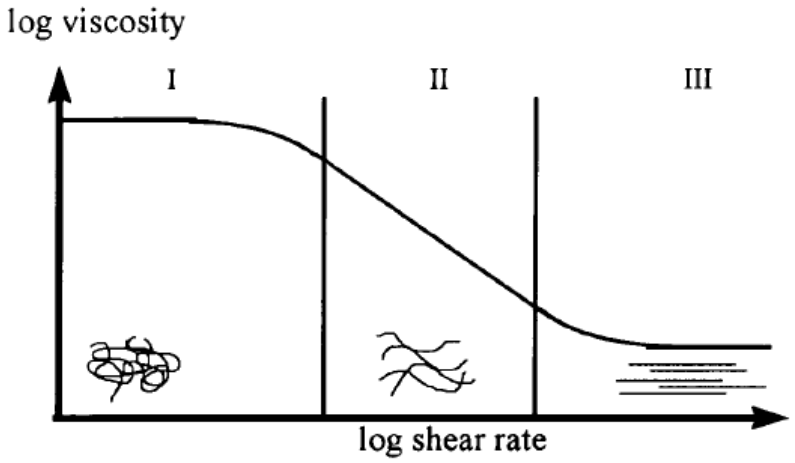

Figure 2, The effect of shear on the viscosity polymeric materials: low Newtonian plateau (I), power law region (II), and upper Newtonian plateau (III).

As the shear rate continues to increase, the polymer chains begin to align in the direction of flow. Since less force (stress) is required to move the polymer melt, the viscosity decreases. Higher shear rates further align the polymer chains and the viscosity decrease eventually becomes proportional to the increase in the shear rate. In this power law region, the viscosity and shear rate are related by

$$\eta = \kappa \dot{\gamma}^{n-1} \tag{2.1}$$

$$\eta = \kappa \left(\frac{dv_1}{dx_2}\right)^{n-1} = \kappa \left(\frac{V}{h}\right)^{n-1} \tag{2.2}$$

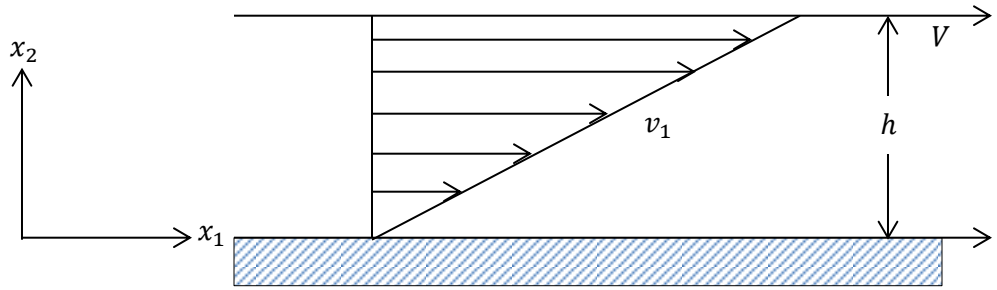

Figure 3, Simple shear flow between parallel plates

where κ is the consistency index and n is the power law index. The *power law index* is an indicator of a material's sensitive to shear (rate), or the degree of non-Newtonian behavior. For Newtonian fluids $n = 1$, for pseudoplastic fluids $n < 1$, with smaller values indicating greater shear sensitivity. At very high shear rates, the polymer chains are, in theory, fully aligned in the direction of flow. Thus the viscosity cannot decrease further and is constant in the upper Newtonian plateau.

The shear rate varies considerably with processing method (see Table 1). Therefore, the degree of alignment, shear thinning, and material relaxation varies considerably with the process. Compression and rotational molding typically induce very little alignment of the polymer chains, and, thus, produce low levels of orientation and retained stress.

Process	Shear rate, s^{-1}
Compression molding	1–10
Calendering	10–100
Extrusion	100–1,000
Injection molding	1,000–100,000

Table 1, Typical Shear Rates for Selected Processes

In contrast, the polymer chains are highly oriented during injection molding, and such parts exhibit high levels of residual stress (5).

2.3.Orientation, relaxation and shrinkage

Since plastic melts expand upon heating, the melt density ρ_m, is related to the solid density by

$$\rho_m = 0.8\rho \tag{2.3}$$

Plastics melts are also compressible. Thus, a temperature and pressure change of 200°C, and 50 MPa, respectively, causes a 10 to 20 percent difference in density, depending on whether the polymer amorphous or semicrystalline. *Specific volume, v*, the inverse of density, is often used to relate density to temperature and pressure. As shown in the typical pressure-volume-temperature (pvT) curves presented in Figure 4, specific volume increase with temperature but decrease with increasing pressure. The isobars exhibit significant changes as the polymer passes through its transition temperature; this is T_g for amorphous polymers and T_m for semicrystalline materials.

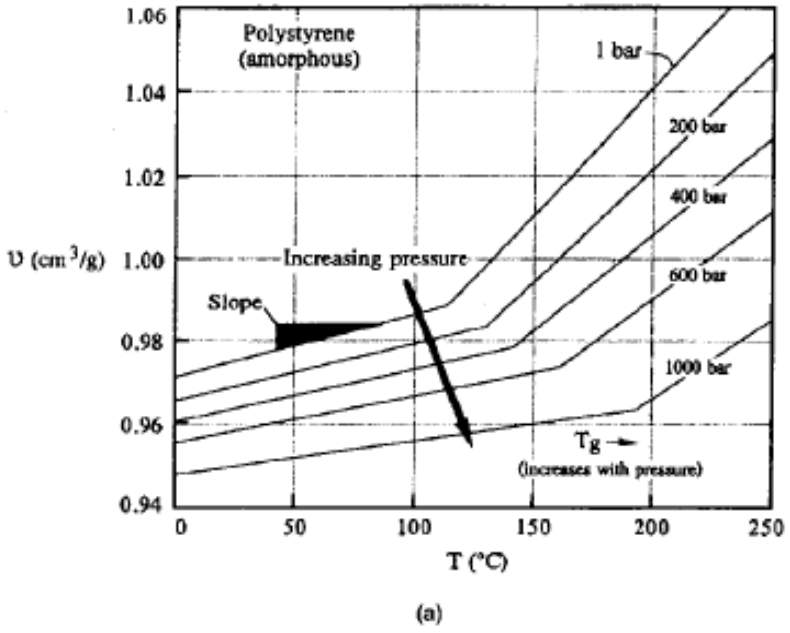

(a)

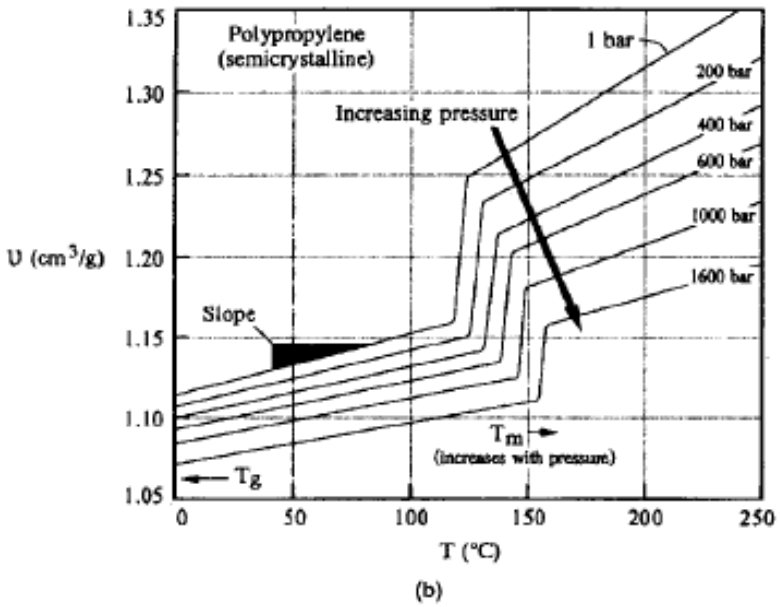

Figure 4, Typical **pvT** curves for: (a) amorphous and (b) semicrystalline polymers.

When cooling semicrystalline polymers, the large reduction in specific volume at T_m is due to the formation of tightly packed regions (crystallites). Increasing pressure shifts the transition shift higher temperatures as the pressure increases, while rapid cooling not only increases T_g and T_m, but also produces higher specific volume below the transition temperature. With relaxation, molecular rearrangement decreases this specific volume. Consequently, annealing time and temperature affect density.

A polymer's dimensional changes are quantified using expansivity or coefficient of (volumetric) expansion (β *or* α_v) and the coefficient of linear thermal expansion (α *or* $CLTE$). Since the volumetric expansion and shrinkage are typically determined from pvT data, they are relatively isotropic. Thus, in theory, linear and volumetric expansion are related by

$$\alpha = \frac{\beta}{3} \tag{2.4}$$

In practice, linear thermal expansion and shrinkage are influenced by orientation of polymer chains during processing. In their totally relaxed state, such as occurs in a solution or un-sheared polymer melt, the individual polymer chains fold back upon themselves and entangle with other polymer chains. Since this random coil Fig. 5a, requires the least energy, it is the preferred conformation. During processing, polymer molecules align in the direction of flow, as shown in Fig. 5b. *This flow-induced orientation* is limited in low-shear processes, such as rotomolding, but severe in high-shear processes like injection molding. However, the oriented chains orientation will, if given the opportunity, return to their random coil conformation. This tendency produces anisotropic shrinkage in plastic parts, die swell, and molded-in stress.

As highly oriented chains relax, they produce greater shrinkage in the direction of flow than in transverse (perpendicular) direction.

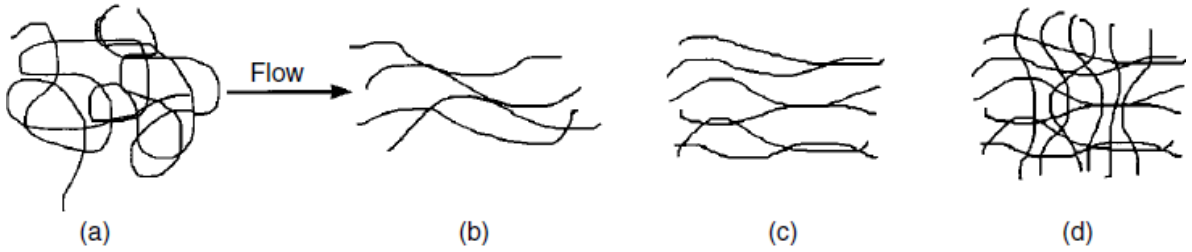

Figure 5, (a) Random coil, (b) Flow-induced orientation, (c) Uniaxial orientation, (d) Biaxial orientation.

If the resin contains glass or other fibers, these also align with the polymer flow. However, since these fibers cannot relax, they constrain the polymer chains, and, thus, limit shrinkage in the flow direction. In such materials, transverse shrinkage is usually greater than shrinkage in the flow direction. When the polymer is cooled so

rapidly that the polymer chains do not have sufficient time to relax, this orientation produces retained or molded-in stress.

Alignment of the polymer chains improves plastics' properties. During extrusion, uniaxial orientation on Figure 5c), is often increased by drawing the extrudate after it exist the die; this enhances mechanical strength in synthetic fibers and flat film. Biaxial orientation on Figure 5d), which occurs in both the flow and transverse directions, produces high strength in blown film and stretch blow-molded bottles. The orientation and relaxation of polymer is also used for products such as strapping, heat-shrink tubing, and packaging film (5).

2.4. Glass Transition Temperature (T_g)

Amorphous polymers are composed of coiled or strained coiled chains, randomly packed, characterized by a major second-order transition, the glass transition temperature reported as T_g. Below T_g, the chains are rigid, above it, flexible and, of course, ever changing in conformation due to thermal motions. Figure 6, shows the specific volume of amorphous polymer. The specific volume values at various temperatures indicate strength of secondary bonds.

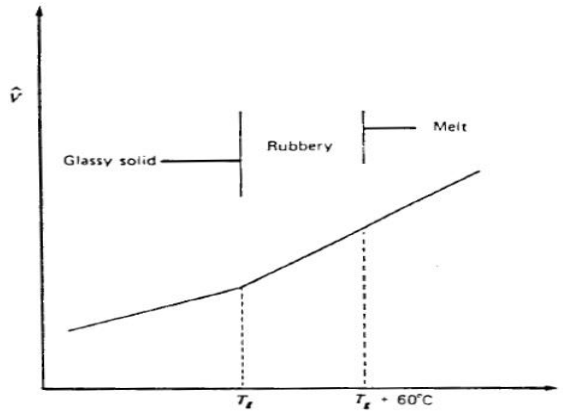

Figure 6, Temperature dependence of the specific volume of amorphous polymer.

Other way to detect when the T_g take place is shown in the Fig. 7, where amorphous polymer soften gradually with increasing temperature and do not have a true melt temperature (because the polymer molecules are randomly dispersed at all temperatures). At low temperatures, amorphous polymers are rigid or glassy. At a critical temperature, or more appropriately, over a narrow temperature range, amorphous polymers start to become flexible or leathery. T_g, is associated with significant polymer chain segmental movement and mobility. At temperatures above T_g, the polymer become rubbery and remains rubbery until temperature becomes high enough that true liquid-like flow is achieved (i.e. processing temperature).

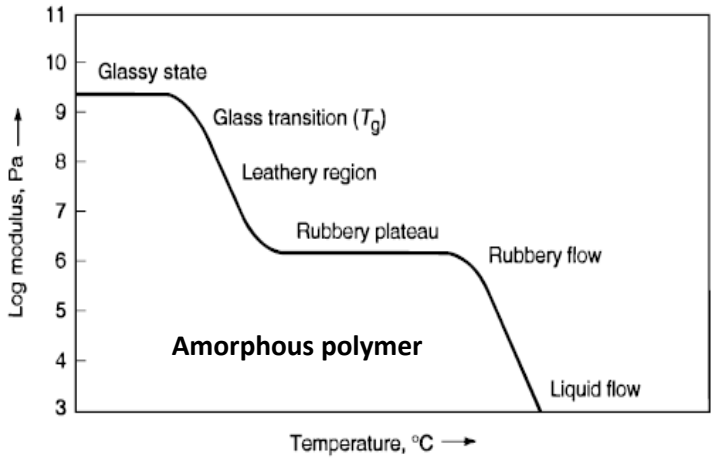

Figure 7, Relationship between elastic modulus and temperature **(5)**.

2.4.Residual Stress in Thermoplastics Parts

Residual stresses are defined as those stresses that remain in a material or body after manufacture and material processing in the absence of external forces or thermal gradients. It is clear that a right understanding of residual stresses is essential

to predict the dimensional and shape stability of a product under different environmental condition. The origin of the residual stresses is associated with two sources. Firstly, the normal stress in the molding process is originated by the viscoelastic nature of the polymeric melt that develops during the filling, packing, and holding state. This normal force is relatively small but is important for large molecular orientations that occur in the PCL injection process. Secondly, thermally induced stresses are originated by non-uniform cooling in the molding part. This last phenomenon takes place due to a rapid increase in the rigidity of the material as it passes through the glass transition temperature, T_g; as a consequence, a highly non-uniform temperature distribution exists across the product. Residual stresses develop during most manufacturing processes involving material deformation (shear deformation), heat treatment, machining or processing operations that transform the shape or change the properties of a material. They arise from a number of sources and can be present in the unprocessed raw material, introduced during the manufacturing or arise from in-service loading.

For instance, the presences of tensile residual stresses in a part or structural element are generally harmful since they contribute to, and are often the major cause of, fatigue failure and enable the ingress of chemical through micro-cracks and by consequence provoke serious damage to the part. Compressive residual stresses induced by different means in the (sub) surface layer of material are usually beneficial since they prevent origination and propagation of fatigue cracks, and increase wear corrosion resistance due to chemical attack and abrasion.

It is very important to consider the problem of residual stress a complex problem including, at least, the stages determination, analysis, and beneficial distribution of residual stresses. The analysis include the following main stages

Stage 1. Residual Stress determination:

- Destructive and nondestructive techniques.

Stage 2. Analysis of residual stress effects:

- Experimental studies.
- Computation.

Stage 3. Residual stress modification (if required):

- Application of stress-relieving techniques.
- Change in technology of manufacturing/assembly.

The three stages are considered in this work, with emphasis on destructive and nondestructive determination, experimental studies and application of stress-relieving techniques, their results will be showed in the next chapters. Over the last few decades, various quantitative and qualitative methods for residual stress analysis have been developed. In general, a distinction is usually made between destructive and nondestructive technique for residual stress measurement (14).

2.4.1. Nondestructive method of residual stress measurement

The term nondestructive testing is applied to test or measurement carried out without harming or altering the properties of the part. Quite often, in order to make measurements or to study certain characteristics of a part, it becomes necessary to destroy the integrity of the part. Nondestructive testing methods allow one to determine flaws, imperfections, and nonuniformity without destroying the part.

Nondestructive tests range from simple visual examination, weighing, and hardness measurement to more complex electrical, ultrasonic, and optical, etc. The discussion on nondestructive testing in this chapter is confined to optical measurements (15).

2.4.2. Photoelasticity Technique

The discovery of photoelasticity effect is accredited to Sir David Brewster who in 1816 published an account of his finding that clear stressed glass when examined in polarized light exhibited color patterns. There are two convenient ways to describe the propagation of the light and its interaction with materials, which are: electromagnetic wave model and quantum model. For most practical purpose, light (including infrared, ultraviolet and radiowaves) can be considered to be energy in form of electromagnetic waves. At any time, the wave train of radiation can be completely described by two vectors that perpendicular to the direction of travel of the ray and perpendicular to each other. These vectors are: electric and magnetic, which exist simultaneously in planes at right angles such that the line intersection of planes is parallel to the direction of the light ray. The term polarization commonly used in this work to imply that some kind of control over light vector exists. However ordinary light without any polarizer has the behavior show in the Figure 8.

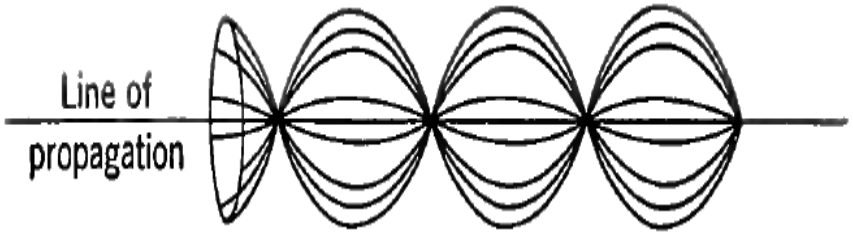

Figure 8, Ordinary Light –No control over light vector

On the other hand, light is said to be plane-polarized when the light vector is confined to a single plane. The plane contain the light vector is known as the plane of vibration, and the plane at right angles is plane polarization as we can see in the Figure 9, (16).

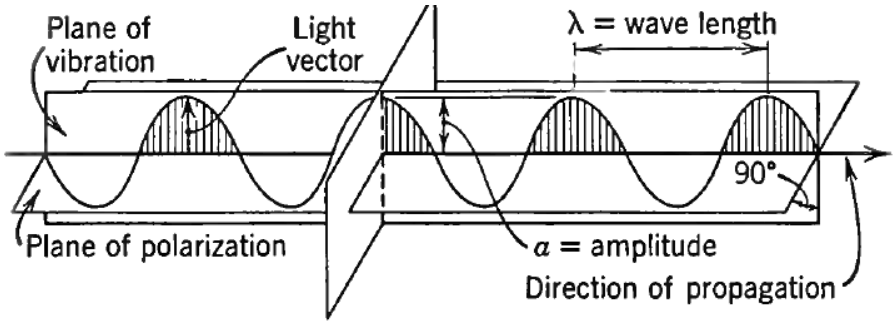

Figure 9, Plane polarization

In photoelasticity is possible to see a range of band color usually called monochromatic lines which possessing different frequencies and can be distinguished from one to another through the sense of color. In the case of visible light the entire range of colors can be seen in the spectrum from a frequency of proximately 390 nm (deep red) to 700 nm (deep violet). Figure 10, is a chart of electromagnetic spectrum showing the various divisions (17).

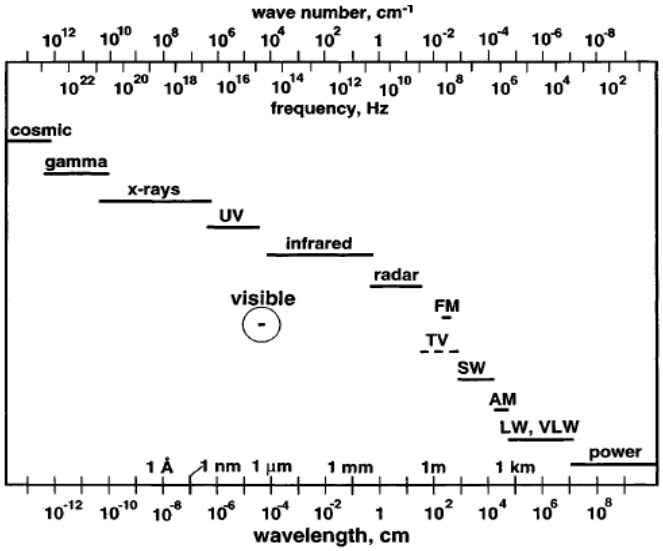

Figure 10, The electromagnetic spectrum.

The electromagnetic spectrum covers an extremely broad range, from radio waves with wavelengths of a meter or more, down to x-rays with wavelengths of less than a billionth of a meter. Optical radiation lies between radio waves and x-rays on the spectrum, exhibiting a unique mix of ray, wave, and quantum properties. At x-ray and shorter wavelengths, electromagnetic radiation tends to be quite particle like in its behavior, whereas toward the long wavelength end of the spectrum the behavior is mostly wavelike (18). The visible portion occupies an intermediate position, exhibiting both wave and particle properties in varying degrees.

These individual wave lengths or monochromatic lines may be plane-, circularly, or elliptically polarized. White or polychromatic light consists of a mixture of light of several wave lengths. The intensity of the light is proportional to the square of the amplitude of vibration.

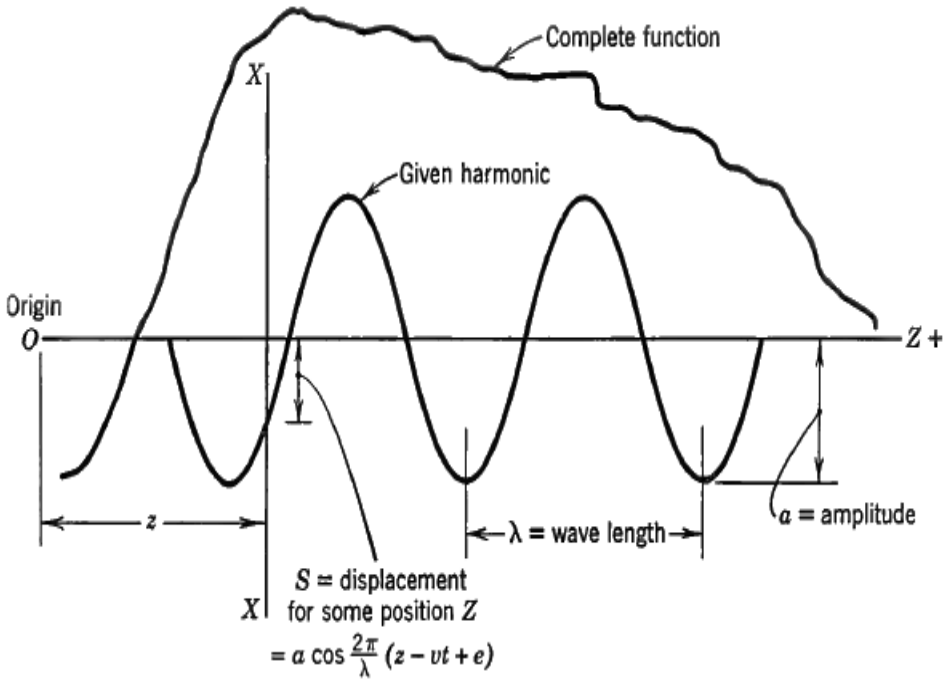

Figure 11, Mathematical representation of light wave **(16)**.

When light passes from one medium into another of different density, there is a change in velocity. The ratio of these velocities is called the index of refraction. Thefore,

$$Index\ of\ Refraction = \frac{Velocity\ in\ 1st\ medium}{Velocity\ in\ 2nd\ medium} \tag{2.5}$$

Since the light is considered as composed of waves, its individual components may be represented mathematically in the form,

$$S = a\ cos\frac{2\pi}{\lambda}(z - vt_s + e) \tag{2.6}$$

as illustrated diagrammatically in the Fig. 10. A complicated condition can be expressed by the combination of an infinite number of elements such that

$$S = \sum_{i=1}^{i=\infty} a_i\ cos\frac{2\pi}{\lambda_i}(z - v_i t_s + e_i) \tag{2.7}$$

Where

S= magnitude of the displacement given by vector

z= distance along the light ray from some reference point

v= velocity of propagation

t_s= time

e= a constant

In the case of monochromatic light is under the special circumstance in which $z\ and\ e$ both happened to be zero, equation reduce the simple form,

$$S = a\ cos\frac{2\pi v}{\lambda}t = a\cos(2\pi f)t_s \tag{2.8}$$

This shows that the magnitude of the displacement indicated by light vector varies harmonically with time, and the light has a color dependent on the frequency (19).

2.4.3. Fundamental Optical Laws of Photoelasticity

Almost all transparent materials such as glass, celluloid, Bakelite, and many other synthetic resins temporarily have to some extend the same optical effect on a beam of light as a crystal when these materials are subject to stress. Photoelasticity is based on the phenomenon of birefringence, which denotes anisotropy due to strained transparent material and as a consequence the index of refraction, n, it becomes directional. In this case the transmission of light through strained materials obeys the following two laws, which form the basis of photoelastic stress determination:

1. The light is polarized in the direction of the principal-stress axes and is transmitted only on the planes of principal stress.
2. The velocity of the transmission on each principal plane is dependent on the intensities of the principal stresses in these two planes and the difference of the refraction index given by the following equations:

$$\begin{aligned} \delta_1 &= n_1 - n_0 = A\sigma_1 + B\sigma_2 \\ \delta_2 &= n_2 - n_0 = A\sigma_1 + B\sigma_2 \end{aligned} \tag{2.9}$$

where δ_i refers to the refraction index on the I axes,

n_0 is the refractive index of unstressed material,

$n_1 =$ the refractive index on principal plane no. 1,

$n_2 =$ the refractive index on principal plane no. 2,

σ_1 and $\sigma_2 =$ the principal stresses,

A and B = the photoelastic constants of the material.

In this case, the difference between the refractive indices on the principal planes is given by the equation

$$\delta_1 - \delta_2 = n_1 - n_2 = (A - B)(\sigma_1 - \sigma_2) = C_B(\sigma_1 - \sigma_2) \quad (2.10)$$

where C_B is the differential-stress optical constant.

As a result of their velocity difference, the waves vibrating along two principal planes will emerge out of phase, and their relative distance, or retardation, δ, is given by:

$$\delta = (n_1 - n_2)t = C_B t(\sigma_1 - \sigma_2) \quad (2.11)$$

or

$$n = \frac{\delta}{\lambda} = \frac{C_B t(\sigma_1 - \sigma_2)}{\lambda} \quad (2.12)$$

where t is the thickness of material crossed by the light and λ is the wavelength of light (570 nm for plastic according to ASTM standards); where the equation expresses the stress-optical law.

2.4.4. Polariscope Arrangement

The device or optical system most frequently employed to produce the necessary polarized beams of light and to interpret the photoelasticity effect in terms of stress is called polariscope. It may take a variety of different forms, depending on the desire used.

The optical equipment used in this analysis to perform the experiments of qualitative and quantitative measurements, were based on two models of arrangement basically:

a) Plane polariscope

b) Plane polariscope with compensator

Both arrangements can be observed on Figure 12, a) and b), respectively. They are equipped by: the light source L, polariscope P, which polarized the light in a right vibration plane, model or sample to be analyzed M, compensator C, used in the arrangement b), which determine the retardation value, δ, the analyzer A, and finally the screen or the person which perform the experiment T.

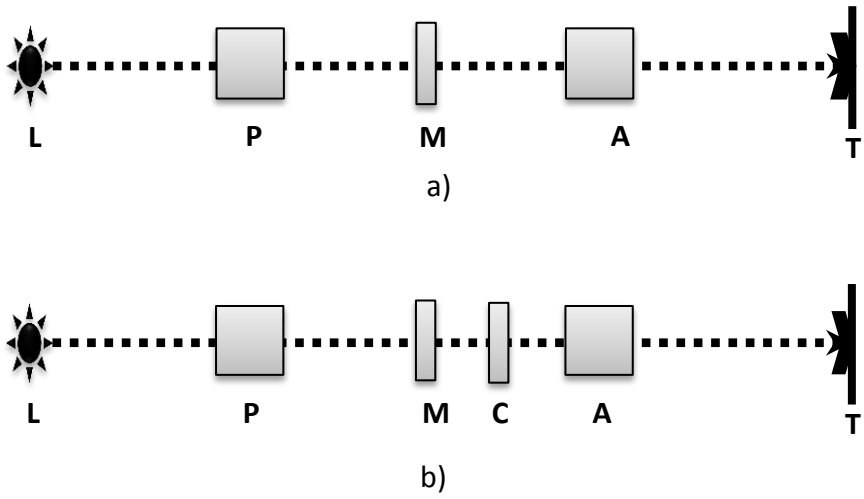

Figure 12, Optical equipment arrangement, a) plane polariscope, b) plane polariscope including compensator to obtain the values of $\boldsymbol{\delta}$.

When light arrives at the model, in general, its plane of vibration will not coincide with either principal planes of stress. Therefore, since the stressed model only transmits

light on the principal planes, the original vibration is immediately resolved into two components as it enters to the model.

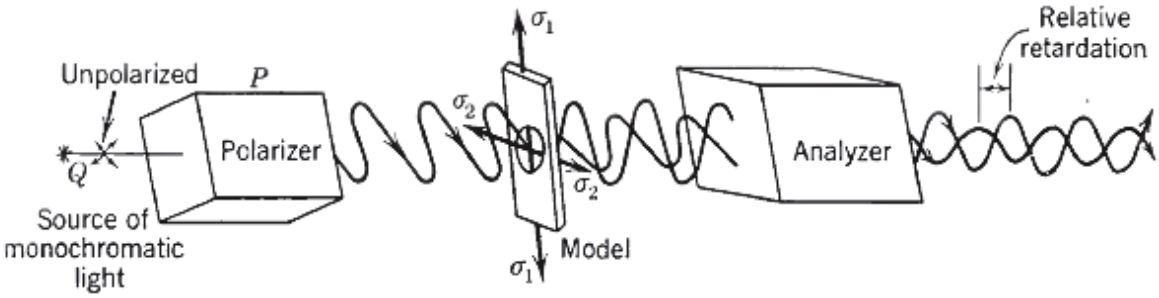

Figure 13, Model in a plane polariscope

For plane polariscope with compensator this is introduced between model and analyzer, for this work was used a compensator model LWC-100 which is a single-wedge compensator (also called quartz wedge or Babinet compensator) made of synthetic crystal materials. The compensator exhibits a linearly-variable retardation and, when observed in polarized light, will show equidistant fringes.

A linearly scale on the compensator permits location of these fringes and calibration. At each point of the compensator, the retardation is known.

When the retardation δ at the point-of-interest (POI) is equal to and opposite in sign (tension vs compression) to the retardation of the compensator δ_c the total becomes zero and a black fringe is observed at the POI.

$$\delta + \delta_c = 0 \tag{2.13}$$

$$\delta = -\delta_c \tag{2.14}$$

Since the retardation of compensator δ_c is known, we can measure δ at any point of specimen (16).

2.4.5. Design of Experiments (DOE)

In industrial applications the way to solve problems is being carried out by the efficient application of scientific principles during the process of refining an existing product or process or by designing a new product or product that has to fulfill with legal and customer requirements. The engineering, or scientific, method is the approach to formulating and solving these problems by the following steps:

2. Develop a clear and concise description of the problem.
3. Identify, at least tentatively, the important factors that affect this problem or that may play a role in it solution.
4. Propose a model for the problem, using scientific or engineering knowledge of the phenomenon being studied. State any limitations or assumptions of the model.
5. Conduct appropriate experiments and collect data to test or validate the tentative model or conclusion made in step 2 and 3.
6. Refine the model on the basis of observed data.
7. Manipulate the model to assist in developing a solution to the problem.
8. Conduct and appropriate experiment to confirm that the proposed solution to the problem is both effective and efficient.
9. Draw conclusions or make recommendations based on the problem solution.

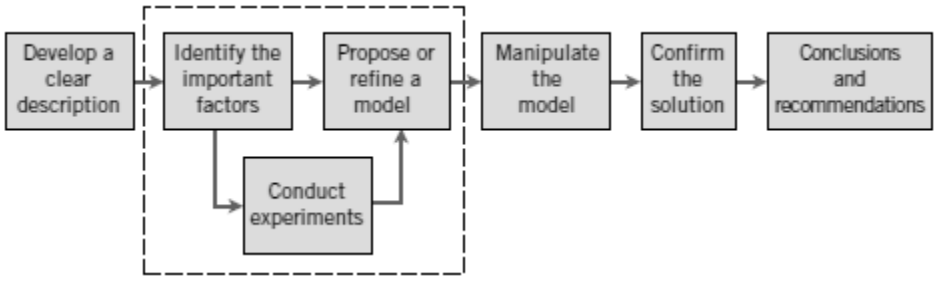

Figure 14, The engineering method. Steps 2–4, are enclosed in a box, indicating that several cycles or iterations of these steps may be required to obtain the final solution

However the statistics deals with the collection, presentation, analysis, and use of data to make decisions, solve problems, and design products and processes. Because many aspects of engineering practice involve working with data.

An experiment is just a test or series of tests. The validity of the conclusions that are drawn from an experiment depends to a large extend on how the experiment was conducted (20).

Factorials designs are widely used in experiments involving several factors where it is necessary to study the joint effect of the factors on a response. There are several special cases of the general factorial design that are important in the research work and have considerable practical value.

The most important of these special cases is that of *k* factor, each at only two levels. These levels may be quantitative or qualitative. A complete replicate of such a design requires a 2k factorial design.

The 2^k design is particularly useful in the early stages of experimental work, when there are likely to be many factors to be investigated. It provides the smallest number of runs with which *k* factors can be studied in a complete factorial design. Consequently, these deigns are widely used in factor screening experiments (21).

The application of the scientific method and statistics were important, for the determination of factors and levels of DOE to minimize the effect of residual stresses on thermoplastic parts which were causing serious damage to the product under series manufacturing.

Chapter III

Experimental Methodology

This chapter details the samples preparation and the experimental methodologies that were employed in this project. In this work, we consider that the ability to predict the lifetime of failure rate would be highly beneficial. Therefore, the plastic part should be tested in real time and in environments similar to those in which the part will be exposed.

The analyzed pieces under investigation in this work were made of polycarbonate (PC) (trade name: Makrolon AL2447) which physically is like a crystal clear. This PC has a low-density and is used for headlamp covers. This also contain a specific scratch-resistant coatings.

3.1.Bulk Samples Preparation

Polycarbonate pellets were molded in an injection molding tool creating plastic cover lenses used in headlamps assembly process. A 1000 tonnage injection molding machine was used to inject lenses with an injection molding tool with a weight of 1145 kilograms, the fixed cavity is shown in the Figure 15, where relevant features of the injection molding tool are shown. Those characteristics marked in the Figure described above play an important role during the molding process.

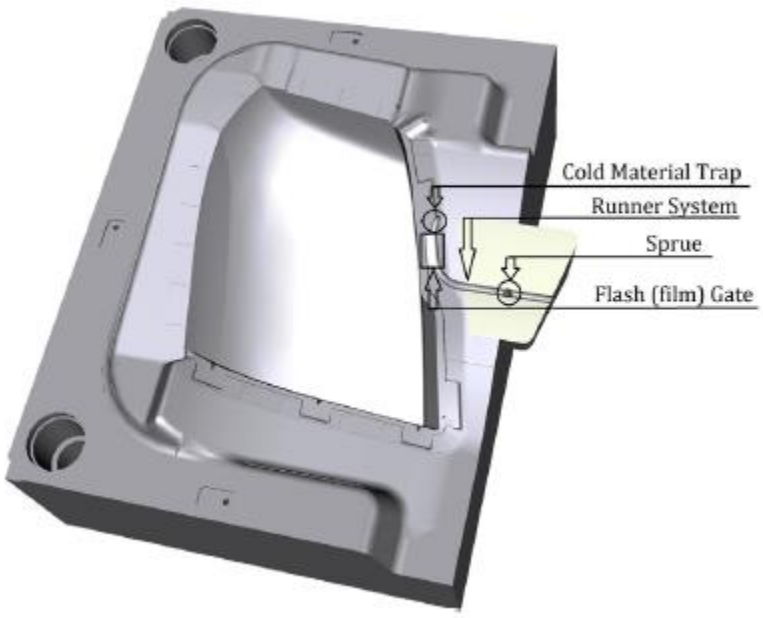

Figure 15, 3DSolid model of PCL's injection molding tool cavity

Concave cover lenses were produced to obtain samples for the experimental analysis carried out in this work and the lens is shown in the Figure 16.

Figure 16, Plastic cover lens subject to analysis

In the table 2, we present the most important process parameters which were took in account during the injection molding process, to produce thousands of plastic cover lenses subject to analysis.

Melt Temperature (°C)	Mold Temperature (°C)	Cooling Time (sec)	Injection Time (sec)	Cycle Time (Sec)
300	MS: 60 FS: 75	35	4.4	72.6

Table 2, Processing conditions used for injection molding

3.2.Experimental Stress Analysis

Following the steps regarding to the analysis of residual stresses mentioned in section 2.4, of this work. First steps for residual stress determination was the characterization by destructive and nondestructive experimental methodologies.

Experimental stress analysis is one of the most versatile methods for analyzing possible failure, in this work chemical and photoelasticity were the experimental methodologies applied in this investigation

3.3.Experimental Stress Analysis: Destructive Characterization

Plastic cover lens made of thermoplastic polycarbonate are known to be highly susceptible to environmental stress cracking when they are exposed to organic compound liquids. This type of failure can be prevented by insuring that the level of mechanical stress on plastic parts is below than the characteristic critical cracking stress for the particular test medium.

The mechanisms by which the test medium contact initiates craze or crack formation can be correlated with the solubility of the test medium in the polymer, due to local deformation zones in the surface and areas close to the surface and hence to weak points (micro-cracks, crazes).

It is possible to use test fluids for estimate of frozen-in stresses in transparent thermoplastic parts where is easy to detect crazes instead of color parts. Test fluids have different "reaction thresholds", which are present in the Figure 17, and they are based on their effect on the molding being tested. The selection of the test medium is a function of the application and the level of security required.

Test medium	Volume ratio	Exposure time (min)	Reaction threshold (MPa)
n-propanol	-	15	> 15
Ethyl acetate and methanol	1:3	15	> 15
Ethyl acetate and n-propanol	1:20	15	> 13
Ethyl acetate and n-propanol	1:10	15	> 11
Ethyl acetate and n-propanol	1:5	15	> 10
Toluene and n-propanol (TnP)	1:10	15	> 9
Ethyl acetate and n-propanol	1:3	15	> 7
Ethyl acetate and methanol	1:2.5	15	> 7
Ethyl acetate and n-propanol	1:2	15	> 6
Toluene and n-propanol (TnP)	1:3	15	> 4
Ethyl acetate and n-propanol	1:1	15	> 4
Propylene carbonate	-	1	> 2

Figure 17, Test medium reaction threshold for testing of parts produced with Makrolon® **(11)**.

If a part is subject to mechanical stressing (e.g. assembled with other parts), the test should be conducted with a test fluid of a mixture of ethyl acetate and n-

propanol; 1:2, In case of bigger external loads, it should be tested with mixture of ethyl acetate and n-propanol, 1:1 or even with propylene carbonate.

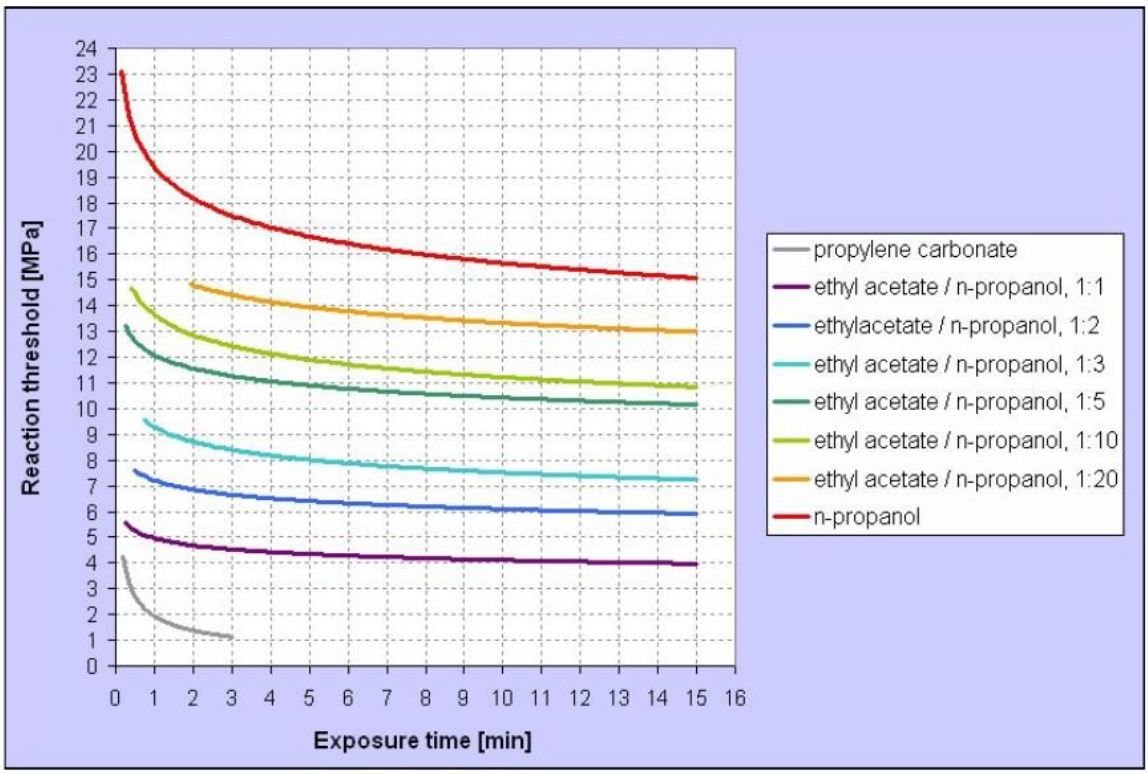

Figure 18, Stress crack test under load to DIN EN ISO 22088-2. Tensile creep method on medium viscosity Makrolon® **(11)**.

On Figure 18, we can see a plot of curves for residual stress determination as function of the exposure time for different test medium. Test fluid used in this work were, ethyl acetate / n-propanol, 1:1 and propylene carbonate. The first one with a reaction threshold of > 4 MPa and with a exposure time from 0 to 15 minutes, the second one (propylene carbonate) with a reaction threshold of > 2MPa and an exposure time from 0 to 3 min.

During the characterization process by using destructive analysis, samples were storage at laboratory for one hour after its manufacturing and tested under controlled temperature room at 23 ± 2 °C. Once the part has been exposure to certain

time, the part was removed and examined visually to determinate the presence of any cracks that may be extended. A chronometer was used to record the exposure time of part under chemicals attack.

3.4.Experimental Stress Analysis: Nondestructive Characterization

Photoelasticity is a full-field; visual technique for measuring stress. This is described in detail on section 2.4. As is shown isotropic plastics exhibit a temporary, double refractive index when they are stressed. The index of refraction changes with the level of stress, making this optical property the basis of the photoelasticity technique.

The polariscope used in this investigation is shown in the Figure 19, it was manufactured by the University of Olomouc.

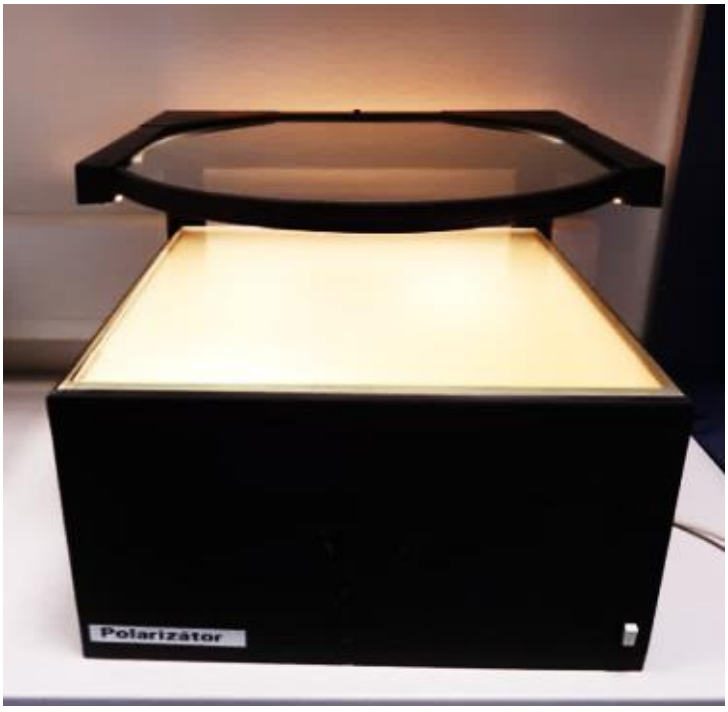

Figure 19, Polariscope used in this work which consists of light source L, and polarizator P.

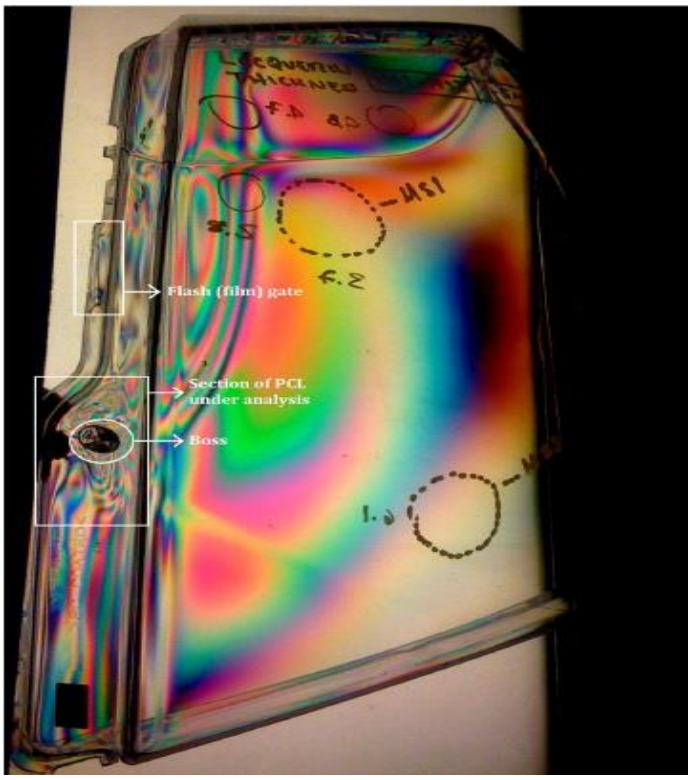

Figure 20, Plastic cover lens analyzed under polarized light where streamlines are detected close to the gate

Rectangular samples for photoelasticity and chemical attack experiments were obtained with the following physical characteristics length 120 mm per wide 95 mm with a wall thickness of 2.8 mm from plastic cover lens where the area of study was located as shown in Figure 21.

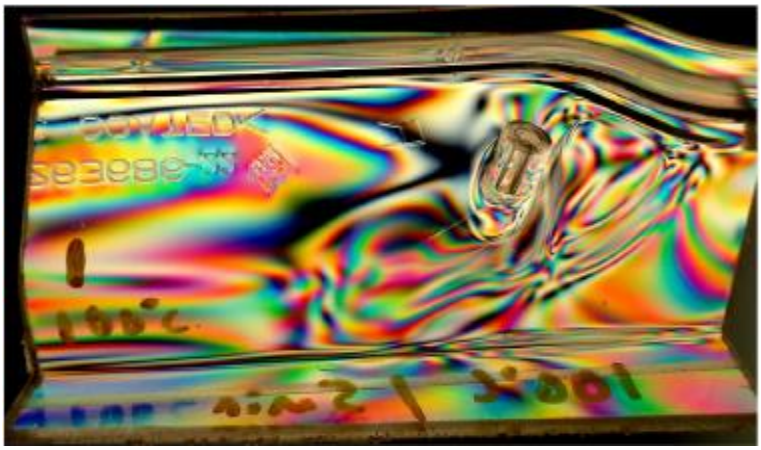

Figure 21, Section of plastic cover lens under polarized light

Regarding to the equipment used to determine the retardation value, it is shown in the Figure 22, model LWC-100 single-wedge (also called quartz wedge or babinet compensator) made of synthetic crystal materials. This compensator exhibits a linearly-variable retardation and, when observed in polarized light, will show equidistant fringes.

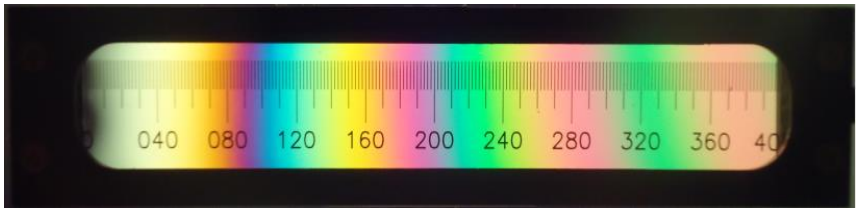

Figure 22, Shown the compensator LWC-100 used to determine the retardation value.

A linearly scale of the compensator permits location of these fringes and calibration. The compensator (model LWC-100) is calibrated using an interferometric filter transmitting a 10-nm band at the "standard" wavelength described in ASTM test methods F218 and D4093 (with a wavelength value of 570 nm for plastics) (Strainoptics™, Inc., USA).

The stress-optic equation establishes that double refraction is directly proportional to the difference in principal stresses, which is equal to the difference between the two indices of refraction exhibited by the stressed material. By knowing the difference in the indices of refraction and the stress-optical or Brewster's constant, it is possible to calculate the difference in the principal stresses. The difference in the indices of refraction can be determined by dividing the retardation value by the material thickness. The stress equation is

$$\sigma_{MPa} = \frac{\delta_{nm}}{(t_{mm})(C_B)} = \frac{(r)(c)}{(t_{mm})(C_B)} = \frac{(N_{fringes})(\lambda)}{(t_{mm})(C_B)} \qquad (3.1)$$

where r is the reading at the point of interest by the compensator model LWC-100, c is the calibration factor supplied by Strainoptics, and N is the fringe order, which can be calculated as follows:

$$N_{fringes} = (r)(c) = \frac{\delta}{\lambda}\left[\frac{nm}{division} \text{ or } \frac{fringes}{division}\right] \quad (3.2)$$

Our interest is mainly focused on the values of retardation (δ) or reading (r), for which maximal or minimal values of N are attained. If $\delta/\lambda = N$, where $N = 0, 1, 2 \ldots$, the interaction between two waves is called constructive interference. On the other hand, if it takes its minimum value, zero in this ideal case, for $\delta/\lambda = 1/2\,,\ 3/2 \ldots$, this situation is called destructive interference and causes dark fringes.

Once the part has been analyzed by plane polariscope Figure 19, it is possible detect the areas where the flow shows a complex path after starting to fill the cavity of injection molding tool IMT through the sprue, area close to the gate where is located the highest concentration of isochromatic lines and residual stress. This is called qualitative analysis and allows us to start with the investigation by the non-destructive technique.

Chapter IV

Results and Discussion

In this sections will be presented the results obtained from characterization by chemical and photoelasticity technique. This is conducted in order to identify the areas of the plastic cover lens where high density of isochromatic lines are located and where cracks appears during manufacturing process of these parts. This qualitative analysis was carried out initially in the complete PCL as shown in Figure 20.

The correlation of results obtained between the chemical and photoelasticity methodologies are also presented. This analysis allow to identify the magnitude of residual stresses and determine the solution of this problem based on a design of experiment for annealing process conducted under certain factor and levels taking as a reference the glass transition temperature of the material with the aim to avoid affect other characteristics the PCL.

4.1 Preliminary analysis of testing results

As mentioned previously, several experiments were carried out on samples in order to identify the failure mode of cracks on a plastic cover lens at supplier plant in Germany, with the aim to understand the mechanism of cracks on PCL and try to replicate this failure at the local Mexican plant for further investigation. The failure of the multiple cover lenses have been described in chapter 3, meanwhile in Figure 23 is shown the analysis by photoelasticity and the effect of the utilization propylene

carbonate. On Figure 23 b) partial cracks on the part under polarized light and c) the crack on the PCL direct view.

a) b) c)

Figure 23, a) sample under polarized light without heat treatment, b) partial crack, c) complete crack of sample real view on PCL.

The use of propylene carbonate was beneficial to determine the origin of the crack. This started where the dome is located in the plastic cover lens being progressive through concentration of residual stresses on the lens section as shown in Figure 24.

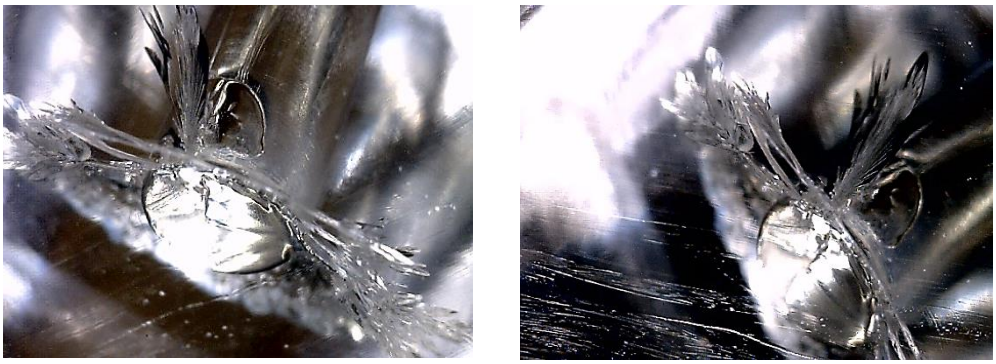

Figure 24. Initial crack originated due to concentration of residual stress where boss is located in the dome.

Based on previous results from experiments, our work was focused in the region close to the dome where was identified a pattern of isochromatic lines.

4.2 Testing results of the polarized light

The stress cracking characteristic of polycarbonate was evaluated by measuring the minimum strain required to produce serious damage to PCLs, Those samples were

then exposed to propylene carbonate, ethyl acetate, and n-propanol, where a non-homogenous region of an isochromatic fringe pattern was identified on the PCLs by qualitative analysis.

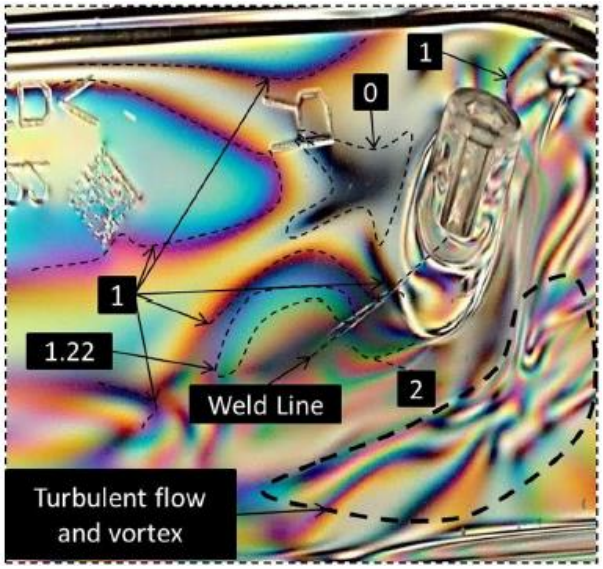

Figure 25, Determination of fringe orders during qualitative analysis

Residual stresses are found to be concentrated in the region where fluid follows a complex path in the mold cavity close to the boss, where a screw is located during the assembly process with other parts. This can be explained by the section change, slider area, and geometrical characteristics of the injection molding tool.

4.3 Testing results of the chemical attack

The chemical attack technique was used to determine the level of internal stress in the microstructural ordering of the polycarbonate, defining those variables involved in the phenomenon of cracking shown in Figure 26, where the failure mode of cracking is a variable that is dependent on exposure time and residual stress level for the chemical used in particular.

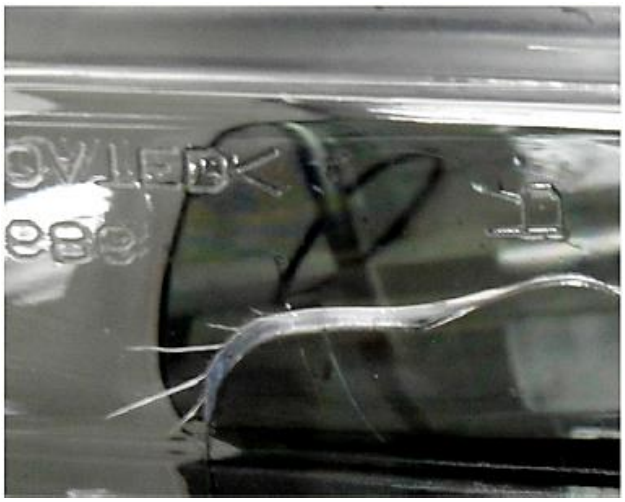

Figure 26, Sample subject to chemical attack by propylene carbonate which cause stress-cracking

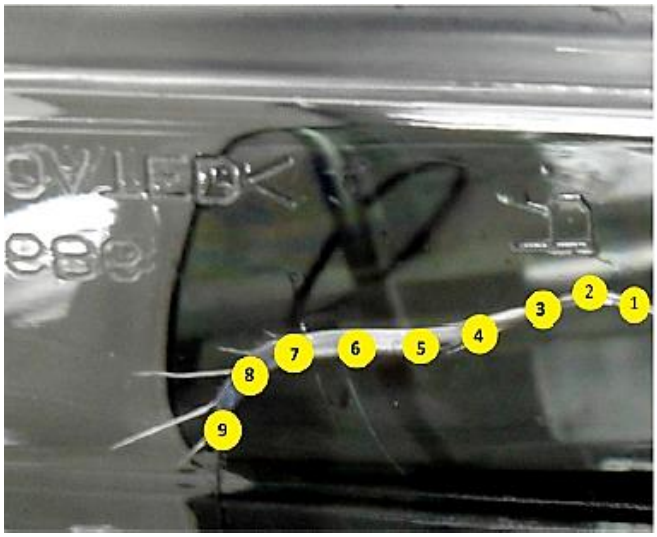

Figure 27, Residual stress magnitude determined as a function of time using chemical attack which causes crack.

Based on that, nine points were defined (1 to 9) in Figure 27, in order to determine the exact period of time when cracks occur at each point after applying propylene carbonate, ethyl acetate, and n-propanol. The results of the chemical attack test were consistent with those identified by photoelasticity, as shown in Figure 28.

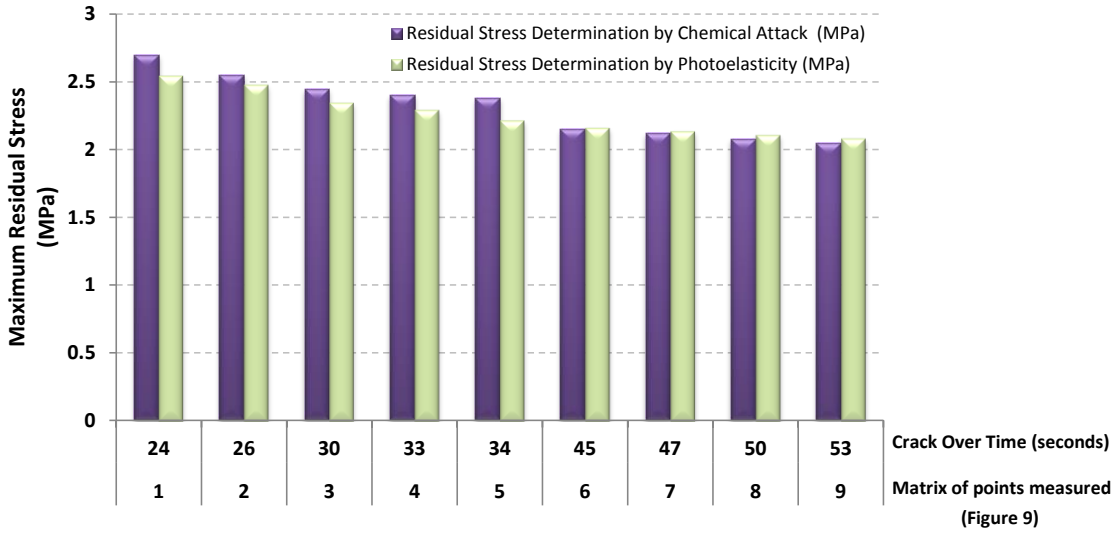

Figure 28, Comparison of results obtained by photoelasticity and chemical attack experiments.

4.4 Testing results after heat treatment

In this work a design of experiments (DOE) was carried out in order to achieve the relaxation of internal residual stresses on PCLs by two different methods of heat treatment. The first method, characterized by batch force hot air (BFHA), carried out and validated in the laboratory. The second method by conveyorized force hot air (CFHA), implemented during series production in the plant once the factors and levels of DOE used by BFHA have been determined.

BFHA consisted of placing PCLs on racks inside an oven in which forced hot air was circulating with the aim to achieve the relaxation of the internal microstructure of PCLs. The start-up of heat treatment by BFHA was conducted according to the DOE 3^2, shown in Table 3. A Memmert brand oven, model 800 D06064, was used in the experiments. Temperature values for DOE were defined based on the Tg = 144 °C for

this commercial PC, and periods of time for the annealing process were established according to values found in the literature.

Temperature of Heat Treatment (°C)	Duration of Heat Treatment (min)		
	5 minutes	12.5 minutes	20 minutes
100°C			
110°C			
120°C			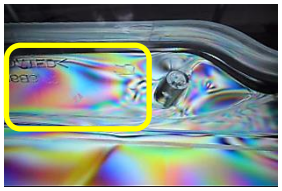

Table 3, Heat treatment process of samples under analysis, using different parameters for temperature and time.

After the termination of the heat treatment is possible to observe on the table 3, that the sample which was subject to the parameters 120°C and 20 minutes showed a visual aspect different to those samples in which the relaxation of residual stress was not effective, the area where the visual aspect has changed is marked with a yellow rectangle where the isochromatic lines on the sample on the left side are very remarkable, meanwhile on the lower right corner the isochromatic lines are more diffuse and the color pattern is smoother as consequence of an effective relaxation of residual stresses.

However, not only the relaxation of residual stresses was the parameter to determine the implementation of the annealing process on series production, in general, after finalizing the experiments for BFHA, four important aspects were evaluated to take the decision about the optimum combination of factors and levels for this DOE.

a) visual damage to PCL

b) proper assembly process of PCL with other parts

c) dimensional stability of PCL

d) relieving of residual stresses in PCL

The results of DOE are shown in Table 3, where the combination of factors and levels which achieve the relaxation of residual stresses was the implementation of heat treatment for 20 minutes at 120 °C.

Experiment	Bloque	Factors		Decision Matrix			
		Time, t (minutes)	Temperature, T (°C)	PCL Visual Damage	PCL Proper Assembly	PCL Dimension Stability	PCL Relieving of Residual Stresses
1	1	12.5	100	o	o	o	x
2	1	20	120	o	o	o	o
3	1	12.5	110	o	o	o	x
4	1	20	100	o	o	o	x
5	1	5	100	o	o	o	x
6	1	20	110	o	o	o	x
7	1	12.5	110	o	o	o	x
8	1	5	110	o	o	o	x
9	1	12.5	120	o	o	o	x
10	1	5	120	o	o	o	x

Nomenclature

o Sucessful result

x Goal no achieved

Table 4, DOE of annealing process

Once the magnitude of temperature and time of the annealing process had been validated by BFHA, the next step consisted in applying the heat treatment by the conveyorized force hot air (CFHA) technique using the combination of factor and level (20 minutes at 120 °C) to thousands of parts in series production. Based on the

complexity of CFHA process, was necessary to carry out the formulation of the hypothesis testing, null and alternative for parts produced in series in two lots, one of them without applying any heat treatment and the other one using the combination of factor and level of the DOE to confirm the effectiveness of heat treatment by CFHA.

H_{null}: There is no significant difference between parts subjected to CFHA and parts not subjected to any heat treatment.

$H_{alternative}$: There is a significant difference between parts subjected to CFHA and parts not subjected to any heat treatment.

Based on the P-value for this hypothesis test, whose results are shown in Table 4, the alternative hypothesis is valid, and it is confirmed that the implementation of heat treatment to PCLs in series production reduces the scrap level and improves the production efficiency of the plant by achieving the relaxation of residual stress in PCLs.

Sampling	Defects	Trial	Proportion	P-Value
No CFHA	194	528	0.36742424	0.0000
CFHA	1	797	0.00125471	

Table 5, Hypothesis tests of proportions for annealing process by CFHA

4.5 Testing results of image processing

In this section, an analysis of image processing was carried out in order to complete the investigation in the field of residual stresses on PCL through a quantitative analysis, by using a technical computing language provided by MATLAB®. Our main

aim in this section is analyze quantitatively the images that were qualitative analysis previously by photoelasticity in section 4.2.

A routine in Matlab was programed using different syntaxes mainly focused in the read of graphics from section 4.2. Samples under analysis in this section were those 27 pictures obtained from the design of experiments 3^2 with 3 replicates after passing through the BFHA. The gradient obtained for each image represents the magnitude of the residual stresses as a function of the color map or isochromatic lines processed for each image.

Figure 29, Section of the sample after BFHA at 110°C and 5 minutes of heat treatment in the laboratory

Section of the picture shown in Figure 29 is an extract of the original image sample subject to heat treatment at 110°C and 5 minutes. This image will be processed by MATLAB®, in order to evaluate the changes in the microstructural ordering of the

molecules in the PCL and by consequence the pattern or distribution of the isochromatic lines which represent the residual stresses remained in the PCL denoted by the vectors in the image.

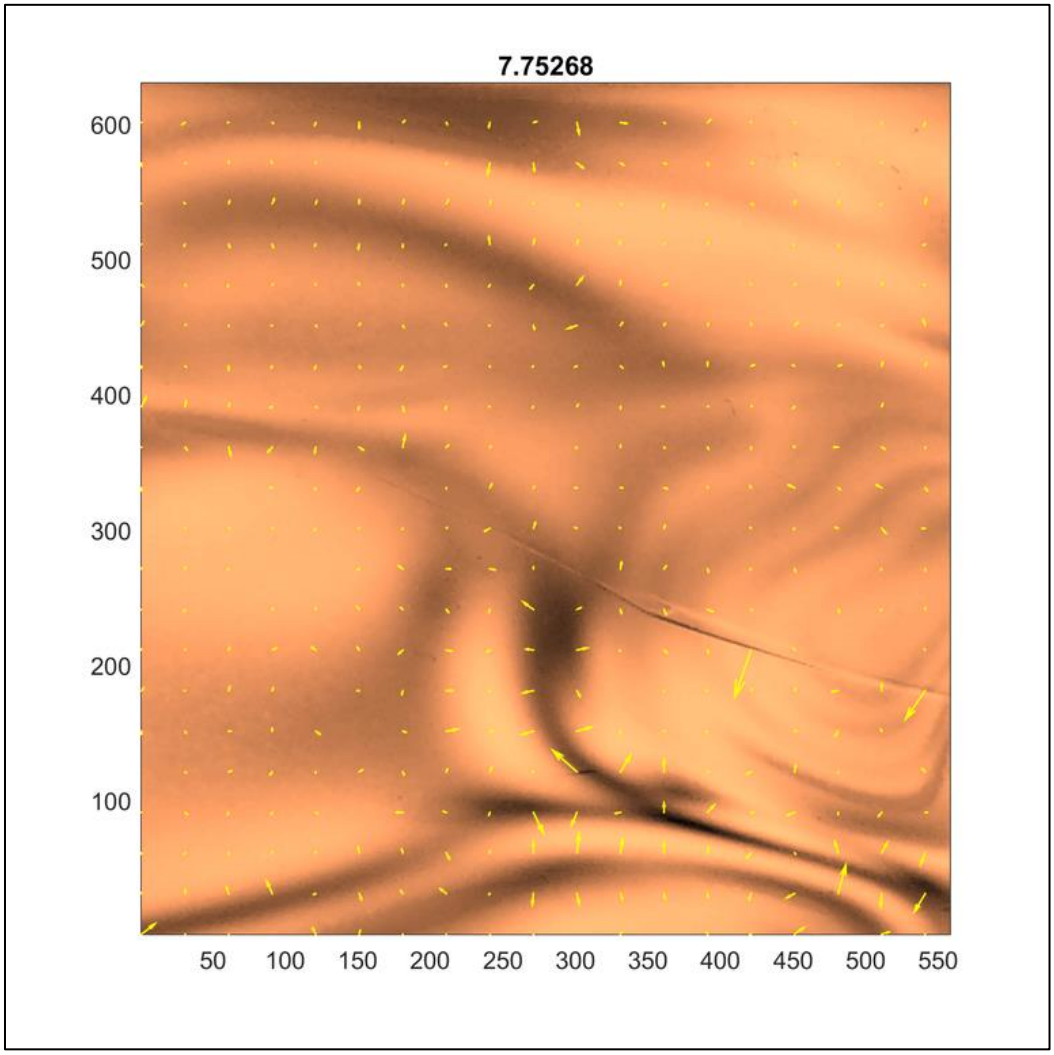

Figure 30, Section of the sample after BFHA at 110°C and 5 minutes processed by MATLAB®.

Result of the image processing can be found in Figure 30, where the vectors which obey a horizontal direction denote residual stress in the PCL. Those results are consistent with the crack over the PCL surface observed in Figure 23 c) where crack obey the horizontal vector pattern.

Table 6, presents the values obtained from the image processing with Matlab, where the quantitative values of the gradient where placed. Those 27 values were obtained from the processed image of the samples used in the DOE with three replicates.

Experiment	Bloque	Factors		Quantitative Analysis
		Time, t (minutes)	Temperature, T (°C)	Gradient
1	1	12.5	110	7.03260858
2	1	5	100	7.93237948
3	1	20	100	7.24131041
4	1	20	110	7.02644484
5	1	5	110	7.72710941
6	1	5	120	7.41254061
7	1	5	110	7.75268193
8	1	20	120	6.49423676
9	1	5	120	7.93012074
10	1	12.5	110	7.20777583
11	2	12.5	100	7.26771607
12	2	20	100	7.08693904
13	2	5	100	7.76211974
14	2	20	120	6.39437114
15	2	20	120	6.14518078
16	2	5	100	7.90402606
17	2	12.5	120	7.08702796
18	2	12.5	120	7.07516671
19	2	12.5	120	6.73655429
20	2	12.5	100	7.21728254
21	2	20	110	7.36349008
22	2	20	100	7.05031578
23	2	5	110	7.74480006
24	2	12.5	100	7.13805943
25	2	12.5	110	7.25994300
26	2	20	110	6.72163173
27	2	5	120	7.36946942

Table 6, Quantitative analysis of residual stresses on samples used in the DOE by image processing.

Table 6, shows the results of the gradient obtained for each experiment carried out after samples were treated by BFHA. By simple inspection of the data in Table 6, it is not easily to identify a pattern or a tendency to the relaxation of residual stresses as a function of temperature and time during the experiments and more when levels of the

factors are randomized. Based on that, the necessity of additional information is important in order to determine if the correlation between factors for the relaxation of residual stresses and stress cracking exist.

Source	SS	df	MS	F	p-value
Block	0.08564	1	0.08564	1.910712	0.180758
Time	3.204734	1	3.204734	71.50077	2.32E-08
Temperature	0.9227	1	0.9227	20.58635	0.000162
Time: Temperature	0.147179	1	0.147179	3.2837	0.083644
Error	0.986061	22	0.044821		0

Number of observations: 27, Error degrees of freedom: 22
Root Mean Squared Error: 0.212
R-squared: 0.827, Adjusted R-Squared 0.795
F-statistic vs. constant model: 26.2, p-value = 4.32e-08

Table 7, Analysis of variance for residual stresses

Table 7, it show the analysis of variance for the table 6. In this case, two effects (Time and Temperature) have P-values less than 0.05, indicating that they are significantly different from zero at the 95.0% confidence level. The R-Squared statistic indicates that the model as fitted explains 82.7% of the variability in emission intensity. The adjusted R-squared statistic, which is more suitable for comparing models with different numbers of independent variables, is 79.5%. Figure 32 shows the Plot main effects of each predictor in the linear regression model, an increase in de time from 5 to 20 min, causes an average decrease of 0.87. In other hand, an increase in de temperature from 100 to 120°C, causes an average decrease of 0.45.

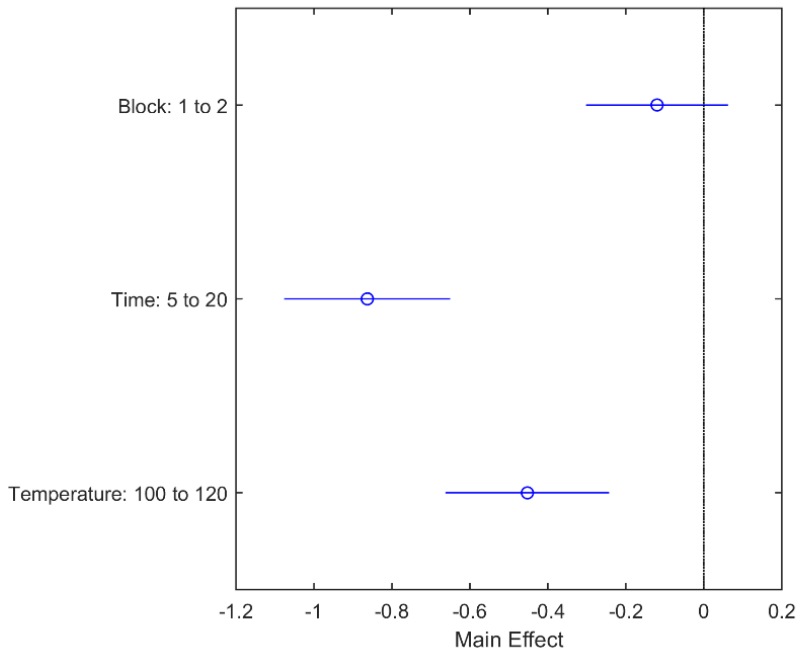

Figure 31, Plot main effects of each predictor in the linear regression model

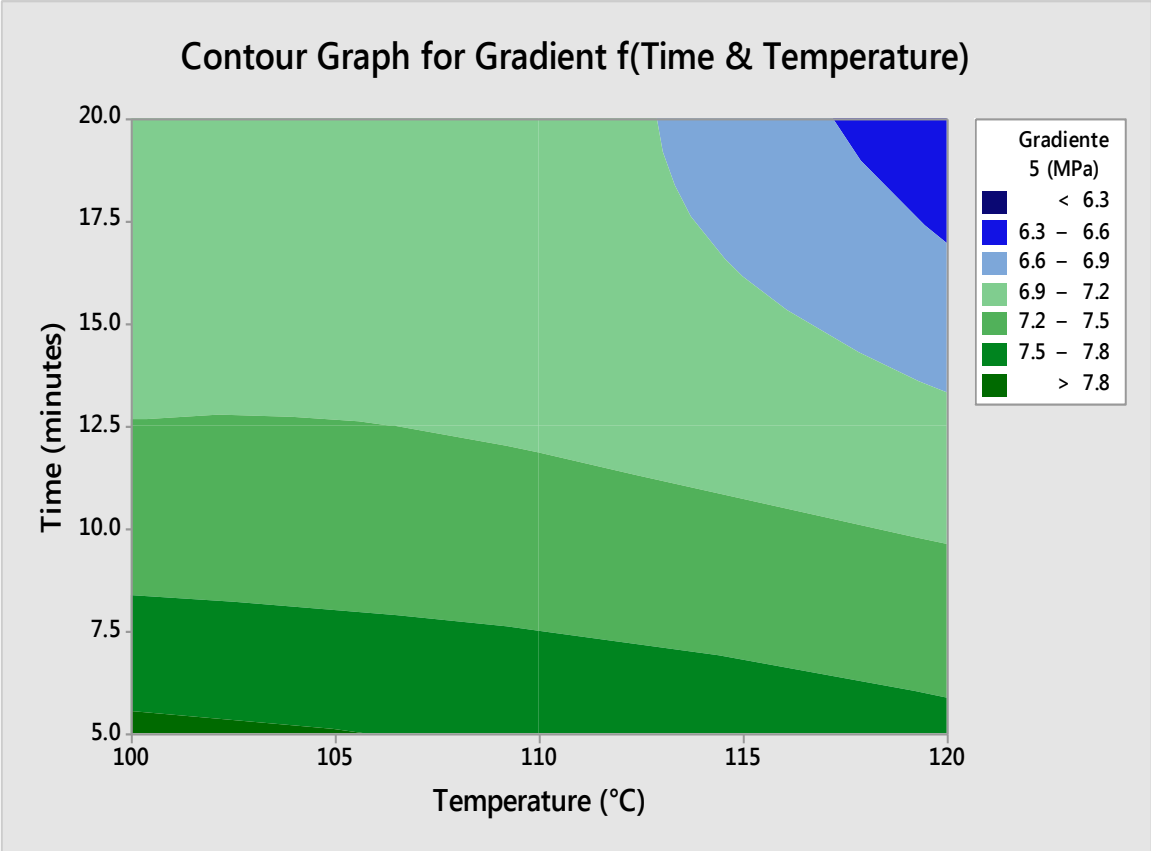

Figure 32, Relaxation of residual stresses as function of [time & temperature].

In resume, the temperature and time are statistically significant; nerveless the time has the double effect in the reduction of stress than the temperature. Because it is industrially important to produce the greatest pieces, in practice the company has to assess whether it is appropriate to use longer heating times.

Additional Figure 32, shows a contour graph in which is able to identify possible correlation between levels of factors regarding the remaining residual stresses in the plastic cover lenses. The design of experiments carried out in this investigation was composed by two factors with three levels each one: One was the time [5, 12.5, 20]min, in which the parts were exposed and the other one was the temperature [100, 110, 120]°C, at what the samples were exposed inside the oven.

The results show that the lowest value of residual stress remain when the combination of levels [120°C and 20min] are crossed, and it is evident that an increase in the values of both factors will cause a relaxation of the microstructural ordering of the PCL for an amorphous polymer.

Due to the residual stresses are related to the difference among the isochromatic lines in the samples. This is based on the fact that samples without residual stresses should not present microstructural structures in these images.

Analysis on the residual stress is present as follows,

The samples under polarized light (see Figure 29) can be associated to the function $z(x, y)$, which represent the monochromatic image (see Figure 30), where x, y represent the pixels of the Figure. Remembering that

The gradient of whatever function is normal to the surface:

$$\nabla z(x,y) = \frac{\partial z(x,y)}{\partial x}\hat{\imath} + \frac{\partial z(x,y)}{\partial y}\hat{\jmath} + \hat{k} \tag{4.1}$$

Then, if the surface does not show structure, the function $z(x,y)$ is a constant, due to this reason the equation 4.1, can be rewrite as follow:

$$\nabla z(x,y) = \hat{k} \tag{4.2}$$

The other case is that the function $z(x,y)$ has a significant structure and the components $\hat{\imath}\ and\ \hat{\jmath}$ are important, due to this reason, the contribution of these variations can be determined by the magnitude of the contribution of $\hat{\imath}\ and\ \hat{\jmath}$ to the gradient, that means

$$f(x,y) = \sqrt{\left(\frac{\partial z(x,y)}{\partial x}\right)^2 + \left(\frac{\partial z(x,y)}{\partial y}\right)^2} \tag{4.3}$$

Equation (4.3) will be zero when the function z, is a constant, which means no residual stresses present on the sample, and will have a maximum for high slopes or maximum stresses.

The function $f(x,y)$ will provide us information about the residual stress in each point of the image. Then the total residual stress in this analysis is defined as follow:

$$Residual\ Stress = \frac{1}{N_x N_y}\sum_{x=1}^{N_x}\sum_{y=1}^{N_y} f(x,y) \tag{4.4}$$

Where $N_x\ \ and\ N_y$ are the pixels of the image processed.

Results shown in this section confirm the previous one obtained by qualitative analysis carried out, with the variant that the results obtained in this section were gotten by image processing as a technique which use a mathematical model computed in MATLAB®, and which let us observe the correlation between high temperatures and long periods of heat treatment for a success relaxation of residual stresses in Figure 32.

However, even when high temperature and long periods are recommended for heat treatment, before decided what levels use is important analyze the T_g of the resin.

Chapter V

Conclusion and Future Work

The presence of residual stress in injection molded parts is of particular concern due to its negative impact on the performance of assembled products like headlights which have to fulfill legal regulations indicated in the norm FMVSS 108, which belongs to National Highway Traffic Safety Administration (NHTSA) from United States of America and which is based on destructive tests.

In this work a successful DOE was applied after the manufacture of Plastic Cover Lenses (PCLs), to achieve the relaxation of the microstructural of the polycarbonate. The relaxation is achieved by heating the PCLs at different temperatures and times. This procedure allows finding the conditions where the service life of the headlights is assured under different environmental conditions. The present work also shows that the thermal treatment in conjunction with the photoelasticity technique is an alternative way of solving and analyzing undesired lenses defects. These are then presented as product quality control.

Additionally, an analysis by chemical attack and photoelasticity shows a good correlation of the results shown in Figure 28, and they can be adopted as a methodology to determine the residual stresses in transparent or translucent materials by performing the following steps: 1) analysis by the photoelasticity model technique 2) identification of zones of high concentration of isochromatic lines, 3) estimation of residual stress by the selected test medium and 4) correlation of the results of nondestructive and destructive techniques.

Finally, results in the present investigation have been validated for destructive and non-destructive techniques used in this work. In the first technique qualitative and quantitative results were obtained by image processing of photoelasticity images. Both techniques represent consistent results.

List of References

1. **Strobl, Gert.** *The Physics of Polymers: Concepts for Understanding their Structure and Behaviour.* Heidelrbeg : Springer, 2007.

2. *Calculation of residual stresses in injection molded products.* **Baaijens, F.P.T.** 1991, Rheologica Acta 30, pp. 284-299.

3. **can, WENG.** Modelling and Simulation of Residual Stresses and Birefringence in the Precision Injection Moulding of Microlens Arrays. 2010.

4. *Residual Thermal Stress in Injection Molded Products.* **ZOETELIEF, W.F.** 1996, POLYMER ENGINEERING AND SCIENCE, Vol. 36, pp. 1886-1996.

5. **Harper, Charles A.** *Modern Plastics Handbook.* United States of America : McGraw-Hill, 2000.

6. *Approximate model of thermal residual stress in injection molded part.* **X. Zhang, X. Cheng, and K.A. Stelson.** 2002, Journal of thermal stresses, Taylor & Francis, Vol. 25, pp. 523-538.

7. *Residual stress distribution in injection molded parts.* **P. Postawa, D. Kwiatkowski.** 1-2, 2006, Journal of Achievements in Materials and Manufacturing Engineering, Vol. 18.

8. *Birefringence technique for characterization of residual stress in injection-moulded micro-lens arrays.* **Can Weng, W.B. Lee, S.To.** 2009, ELSEVIER, pp. 709-714.

9. **Wysgoski, C.H.M. Jaques and M.G.** *Stress Cracking of Plastics by Gasoline.* Dearborn, Michigan : SAE, 1976. 19960229 050.

10. **Yeager, Mark.** *Photoelastic Stress Analysis of Polycarbonate Medical Parts.* Pittsburgh, PA. : Bayer Material Science LLC, 2010.

11. **AG, Bayer Material Sciences.** *Stress crack test - Makrolon® moldings.* Leverkusen, Germany : Global Innovations - Polycarbonates, 2007. PCS-8031.

12. **Dominick V. Rosato, Donald V. Rosato and Marlene G. Rosato.** *Injection Molding Handbook.* Norwell : Kluwer Academic Publishers, 2000.

13. **Anil Kumar, Rakesh K. Gupta.** *Fundamentals of Polymer Engineering.* New York : Marcel Dekker, Inc., 2003. 0-8247-0867-9.

14. **Editor, Sharpe.** *Handbook of Experimental Solid Mechanics.* New York : Springer, 2008.

15. **Shah, Vishu.** *Handbook of Plastics Testing and Failure Analysis.* Canada : John Wiley & Sons, Inc., 2007.

16. **HETENYI, M.** *Handbook of experimental stress analysis.* New York : John Wiley & Sons, Inc., 1950.

17. **Cloud, Gary L.** *Optical Methods of Engineering Analysis.* Cambridge : Cambridge University Press, 1995. 978-0-521-63642-1, 978-0-521-45087-4.

18. **Ryer, Alexander D.** *Light Measurement Handbook.* Newburyport : International Light, 1997. 0-9658356-9-3.

19. **ASTM.** *Standard Test Method for Photoelastic Measurements of Birefringence and Residual Strains in Transparent or Translucent Plastic Materials.* s.l. : ASTM D4093-95, 2010.

20. **Runger, Douglas C. Montgomery & George C.** *Applied Statistics and Probability for Engineers.* New York : John Wiley & Sons, Inc., 2003. 0-471-20454-4.

21. **Montgomery, Douglas C.** *Design and Analysis of Experiments.* Arizona : John Wiley & Sons, Inc., 2001.

22. **Prime, Joseph D. Menczel & R. Bruce.** *Thermal Analysis of Polymers: Fundamentals and Applications.* New Jersey : Wiley, 2009. 978-0-471-76917-0.

23. **Malloy, Robert A.** *PLastic Part Design for Injection Molding: An Introduction.* 2nd. s.l. : HANSER, 2010.

24. *Stress cracking of plastic by gasoline.* **Wyzgoski, C.H.M. Jacques and M.G.** 1976, Society of Automotive Engineers, pp. 18-22.

25. **Polycarbonates, Global Innovations -.** *Stress crack test - Makrolon moldings.* Leverkusen, Germany : Bayer Material Science, 2007.

26. **Jr., M. Joseph Gordon.** *Total Quality Process Control for Injection Molding.* New Jersey : Wiley, 2010.

27. **LLC, Bayer Material Science.** *TnP Solvent Test for Derermining Internal Stresses in Parts Molded of Transparent Makrolon Polycarbonate .* Pittsburgh : s.n., 1999.

28. **Fred W. Billmeyer, Jr.** *Textbook of Polymer Science.* Canada : John Wiley & Sons, Inc., 1984.

29. **Ebewele, Robert O.** *Polymer Science and Technology.* New York : CRC Press, 2000.

30. **William D. Callister, Jr.** *Material Science and Engineering and Introduction.* New York : John Wiley & Sons, Inc., 2007.

31. **Andrew J. Peacock, Allison Calhoun.** *Polymer Chemestry Properties and Applications.* Munchen : Hanser, 2006.

32. *Thermal Processing of Materials: From Basic Research to Engineering.* **Jaluria, Yogesh.** 2003, Journal fo Heat Transfer, Vol. 125, pp. 957-979.

33. **Seitz, J. T.** *The Estimation of Mechanical Properties of Polymers from Molecular Structure.* Midland : The Dow Chemical Co., Central Research, 1992.

34. *Overview Polymer Processing.* **Strutt, J. Vlachopoulos and D.** 2003, Material Science and Technology, Vol. 19, pp. 1161-1169.

35. **Hansen, Donald E. Kline and David.** Thermal Conductivity of Polymers. *Thermal Characterization Techniques.* New York : s.n., 1970, pp. 247-292.

36. **Yaneff, Rose A. Ryntz and Philip V.** *Coatings of Polymers and Plastics.* New York : Marcel Dekker, Inc., 2003.

37. **Campo, E. Alfredo.** *The Complete Part Design Handbook for Injection Molding of Thermoplastics.* Munich : Hanser, 2006.

38. **Gupta, Anil Kumar and Rakesh K.** *Fundamentals of Polymer Engineering.* New York : Marcel Dekker, Inc. , 2003.

39. **Blender, Donald G. Legrand and John T.** *Handbook of Polycarbonate Science and Technology.* New York : Marcel Dekker Inc., 2000.

40. **Gastrow.** *Injection Molds 130 Proven Designs.* Cincinatti : Hanser, 2002.

41. **Soboyejo, Wolé.** *Mechanical Proporties of Engineered Materials.* New York : Marcel Dekker, Inc., 2002.

42. **Mark, James E.** *Physical Properties of Polymers Handbook.* Cincinnati : Springer, 2007.

43. **Sperling, L.H.** *Introduction to Physical Polymer Science.* Canada : Johm Wiley & Sons, Inc., 2006.

44. **Brinson, Hal F. Brinson & L. Catherine.** *Polymer Engineering Science and Viscoelasticity: An Introduction.* Houston : Springer, 2008.

45. **Castellan, Gilbert W.** *Physical Chemestry.* Canada : Addison-Wesley Publishing Company, 1983. 0-201-10386-9.

Biographical Sketch

César Octavio Macías González was born in Colima in 1984. He graduated from the Universidad de Colima, Colima, Mexico in 2006 with his B.S. in mechanical electrical engineering. He started his professional career in Colima working as trainee in Comisión Federal de Electricidad (CFE). One year later he decided to look for a higher academic degree in the Mexico City in order to have a better education. The Heat Transfer and Thermocapillarity of the Instituto Politécnico Nacional, ESIME Azcapotzalco kept his attention and on August 2007 received the opportunity to join this research group in Azcapotzalco, Mexico City.

On August of 2009 César Macías received his specialization degree after doing research on heat transfer in microchannels and on August 2011 received his master's degree after continues with his previous research on heat transfer in microchannels. On January 2016, César has received his Ph.D. degree after doing research on residual stress analysis in thermoplastic parts.

Annex I

During the doctorate studies a scientific research in the field of engineering failure analysis was developed and it was focus on the automotive industrial sector, specifically in the sub-area in the injection molding process.

As product of this research a scientific article was published in the journal of Engineering Failure Analysis 57 (2015) 490–498, by Elsevier. The article was received 8 April 2015, received in revised form 17 June 2015, accepted 13 July 2015 and available online 26 July 2015.

1. *César Macias, et. al., Relaxation of residual stresses in plastic cover lenses with applications in the injection molding process, journal of Engineering Failure Analysis, Elsevier, 2015.*